5. FORWARD CALORIMETER (HF) LAYOUT AND DESIGN

5.1 OVERVIEW AND REQUIREMENTS

5.1.1 Introduction: physics aims

The very forward calorimeter (HF) covers the pseudorapidity range $3.0 \leq |\eta| \leq 5.0$. The front face of HF is located at ± 11.1 m from the interaction point (IP). There are two main objectives with this detector: to improve the measurement of the missing transverse energy (E_T^{miss}) and to enable identification and reconstruction of very forward jets. In some cases, these jets are the distinguishing characteristic of several important physics processes, in others, they are background signatures. With the addition of the HF calorimeters, the total coverage increases to $|\eta| \approx 5$, and this reduces the fake (instrumental) E_T^{miss} by an order of magnitude in the 20-120 GeV energy range over that derived from HB+HE alone.

5.1.2 The HF environment: physics requirements

The physics aims outlined in the previous section have to be fulfilled in a very demanding and hostile environment. To start with, a bunch crossing occurs every 25 ns. With the LHC operating at a luminosity of 10^{34} $cm^{-2}s^{-1}$, and assuming a total *pp* cross section of 100 mb (25 *pp* collisions per bunch crossing), the average particle multiplicity at the IP per crossing is about 5700 (rms=1200). This corresponds to a rate of 2.3×10^{11} s^{-1}, equivalent to 280 particles/crossing/rapidity unit, or 1.1×10^{10} particles/s/unit of rapidity. The most populated region is the inner part of the HF ($4.5<\eta<5$), with an incoming rate of particles of about 9.6×10^{9} Hz equivalent to a flux of about 6.0×10^{6} cm^{-2} s^{-1}. This particle flux will produce absorbed doses that will reach values close to 100 Mrad/year. Therefore, the detectors must be able to survive in an exceptionally high radiation field.

Particles incident on HF will initiate showers leading to large neutron fluxes in the calorimeter absorber (close to 10^{9} cm^{-2} s^{-1} at shower maximum) and to the activation of the absorber material. Thus, the detection technique employed by the HF should be insensitive to neutrons and to low energy particles from the decay of activated radionucleids. As a result of this activation, the inner parts of the HF will be a source of radiation (after 60 days of LHC operation and one day of cooling down) up to about 10 mSv/h. Thus the detector must be robust and require minimal maintenance.

5.1.3 The technique: quartz fibre calorimetry

A charged particle, traversing a quartz fibre with a velocity greater than the speed of light in quartz, emits photons due to the Cherenkov effect. The opening angle of the Cherenkov cone, Θ_C, is related to the speed of the particle, β, and the index of refraction n.

$$\cos \Theta_C = 1/n\beta \quad (1)$$

There is a threshold value ($\beta_{min}=1/n$), below which there is no Cherenkov radiation. The light yield, in photons, due to the Cherenkov effect, depends on α, the fine structure constant, λ, the wavelength of the emitted light, x, is the path of the particle through the medium and z, is the charge of the incident particle.

$$d^2N/dxd\lambda = 2\pi\alpha z^2(\sin^2 \Theta_C /\lambda^2) = 2\pi\alpha z^2/\lambda^2[1-1/\beta^2 n(\lambda)^2] \quad (2)$$

The amount of light observed by a detector positioned at one end of the fibre depends on

the velocity of the particle, on the incident angle, and on the distance between the particle trajectory and the center of the fibre. It also depends on the fibre core and cladding refraction indices, on the spectral transmission range of the fibre and on the spectral quantum efficiency of the light detector.

The particles entering the absorber of a calorimeter produce showers of particles. Those among them which enter a quartz fibre with β close to one are essentially electrons. The electrons producing light in a quartz fibre are roughly those entering the fibre with an angle of $\approx 45^{\circ} \pm 10^{\circ}$ [1].

The immediate implication is that the apparent shower development in quartz fibre calorimeters is dramatically different from the one observed in *dE/dx* calorimeters. The showers appear to be very narrow and, in the case of hadrons, short. A typical transverse shower size for both EM and HAD showers is characterised by the Moliere radius of the absorber.

The Cherenkov effect is insensitive to neutrons (because they have no charge) and to activation products if they lie below the β threshold. In addition, the Cherenkov effect can be considered instantaneous. Therefore there is no other limitation than the photodetectors and electronics which slow down the detector response. Hence, the charge collection is accomplished in much less than 25 ns with the present design.

The HF will be constructed as a block of copper with embedded quartz fibres, running parallel to the beam axis. The photodetectors and associated electronics will be located at the outer parts of the calorimeter, where the radiation doses are lower and these components are easily accessed.

5.2 HF-RADIATION ENVIRONMENT

5.2.1 Shielding requirements and constraints

The large amount of hadronic energy absorbed in the HF inevitably leads to the generation of an immense neutron flux inside of the HF. We observe hadronic leakage from the rear face even after ten interaction lengths. Fortunately, most of the punchthrough is contained within the shielding or is directed towards the end wall of the cavern and does not directly impact any other subdetector. Some of these particles will cross the photomultipliers and front-end electronics. The protection of these devices is the primary reason for quite substantial shielding at the back of the HF. This shielding is also beneficial to the endcap muon system, since the energy carried by the punchthrough particles is converted into neutron and photon albedo at the end wall of the experimental hall, and so indirectly influences the ME4.

For the ME4, radial leakage from the HF is more of a concern than punchthrough. Particles emerging from the HF side faces could directly impinge on the CMS endcap. A substantial effort has been devoted to optimising the shielding configuration around the HF.

The neutron albedo from the HF front face has been shown to be of no importance for the central tracker but, if unshielded, would be an important source of background in the high η region of the endcap muon spectrometer. A 20 cm thick polyethylene slab lining the HF front face is sufficient to suppress the neutron albedo below the level of the neutron flux generated by interactions in the beam pipe.

An important channel for neutron leakage from the HF directly into the ME4 has been

blocked by introducing a 10 cm thick borated polyethylene slab into the endcap/HF interface. The interface itself is designed to be flat, with a clearance not exceeding 3 cm. The lateral faces of the HF are surrounded by 70 cm of shielding elements, of which the innermost 30 cm are steel, followed by 30 cm magnetite concrete with a density of 3.65 g/cm^3. The shielding is completed with a 10 cm thick layer of borated polyethylene. A cylindrical shape shielding is advantageous because of savings in total weight. A shielding structure with square cross section, for example, would leave in the corners some parts of the ME4 directly exposed to the HF.

At the back of the HF we have to deal with the interface to the rotating shielding and shielding the photomultipliers. Behind the HF we have a relatively massive shielding block starting at z=12.95 m. The inner boundary of this block is conical and follows the η=5.3 line. The block has an outer radius of 100 cm and consists of steel and magnetite concrete. Its outer surface is covered by 10 cm of borated polyethylene. The interface to the rotating shielding is provided by a 40 cm of shielding block which is a separate entity that is installed after both the HF and the rotating shielding are in place. The crack between the HF shielding and the rotating shielding shown to be critical. A flat connection is possible if the clearance does not exceed 3 cm. Assuming 3 cm clearance, the rotating shielding starts at z=1496 cm. In addition to its main task of reducing the background in the experimental cavern and ME4, the thin section of the rotating shielding plays a non-negligible role in shielding the HF photomultipliers. The optimization of the rotating shielding design in view of the ME4 is still in progress. Here we use the best design so far, consisting of three radial layers: 30 cm of steel starting at r=20 cm, followed by 30 cm of magnetite concrete and a 10 cm of borated polyethylene, giving an outer radius of 90 cm.

The photomultipliers are stacked between the cylindrical shielding block and the outer lateral shielding described above. To suppress the fluence of punchthrough particles, a special shielding consisting of 5 cm steel, 25 cm borated polyethylene and 10 cm steel is placed between the HF and the photomultipliers. The light from the fibres is fed to the photomultipliers through air-core light mixers that are located in small holes in this shielding.

5.2.2 Results of radiation simulations

We have calculated the particle fluences and radiation dose in a glass plate representing the photomultiplier windows. The results are collected in Table 5.1 and the radial dependence of fluences and dose are shown in Fig. 5. 1 and Fig. 5. 2. Along with the FLUKA results, we provide some values obtained with the MARS code. In general, we observe very good agreement. The increase of the MARS neutron fluence estimate with respect to FLUKA at large radii may be explained by the significantly longer scoring bins (along z) used in MARS.

Table 5. 1

Particle fluences in cm^{-2} and dose in Gy in the position of the photomultipliers of the HF. All values are for an integrated luminosity of 5×10^5 pb^{-1}.

	FLUKA	MARS
All neutrons	2.8×10^{12}	-
Neutrons $E > 100$ keV	2.3×10^{12}	2.9×10^{12}
Thermal neutrons	8.3×10^{9}	-
Charged hadrons	3.8×10^{10}	2.0×10^{10}
Dose	70	-

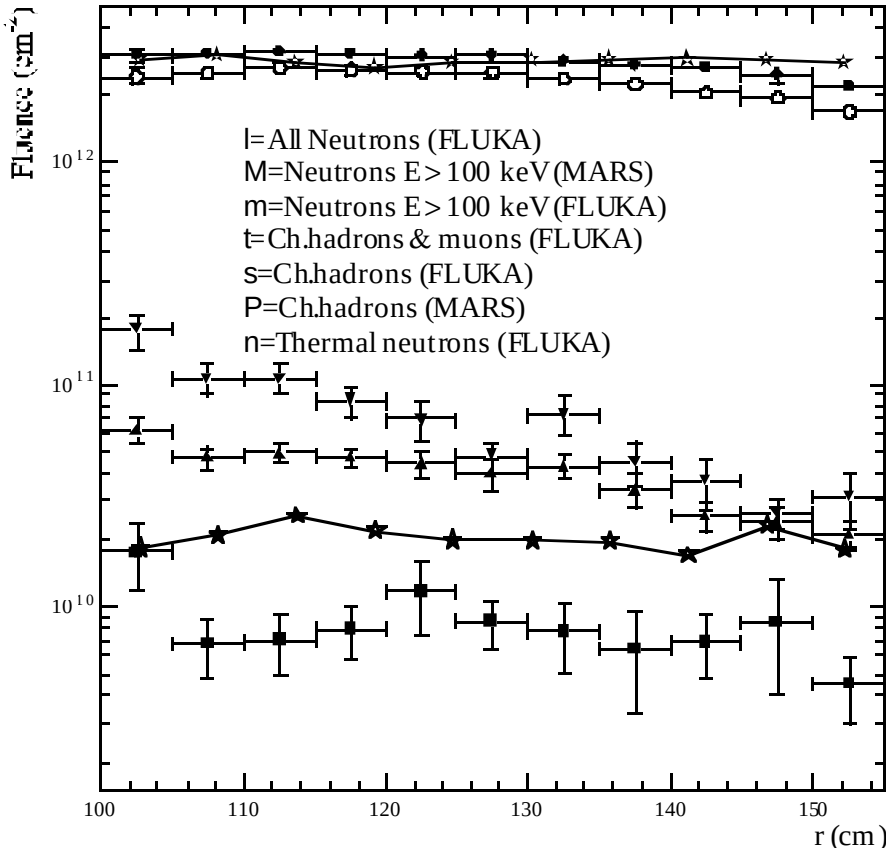

Fig. 5. 1: Fluence of different particle types at the position of the photomultipliers as a function of radius. Values are for 5×10^5 pb^{-1}. The legend (top to bottom) refers to largest to smallest values.

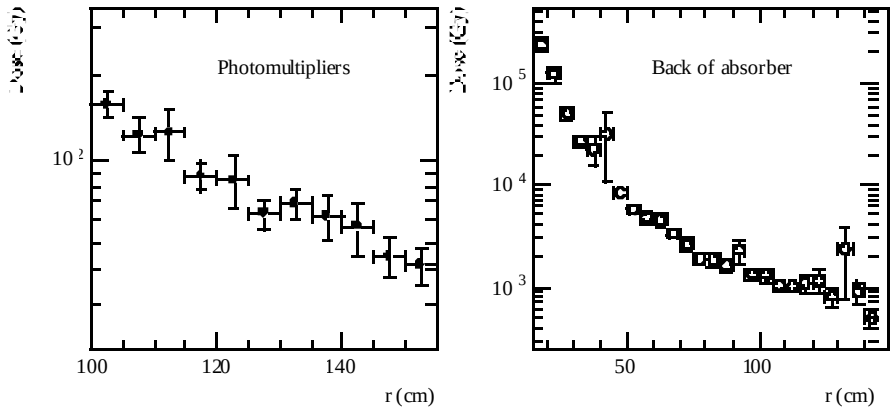

Fig. 5. 2: Radiation dose in the photomultiplier windows (glass) and just behind the absorber (air) as functions of radius. Values are for 5×10^5 pb^{-1}.

Fig. 5. 3 and Fig. 5. 5 show the photon and neutron spectrum in the position of the photomultipliers and behind the HF absorber. We observe that, as expected, the polyethylene has removed a significant amount of the neutrons around 1 MeV and therefore lowered the potential bulk damage to silicon devices. When interpreting the photon spectra, it should be remembered that photons emitted in radioactive decays are not included in the simulation.

Fig. 5. 2 and Fig. 5. 4 show the dose and particle fluences as a function of radius just behind the HF absorber. We can observe a variation by several orders of magnitude between the innermost and outer radii.

Fig. 5. 5 shows the photon and neutron spectrum just behind the HF absorber averaged between radii of 20 cm and 60 cm. The neutron spectrum shows the typical shape inside or on top of pure metal, with very few thermal neutrons (probably backscattered from the polyethylene on the shielding plug) and a very pronounced 1 MeV evaporation peak. The smaller peak around 100 MeV is the more significant one, since these neutrons are very penetrating. Note that the increase of the absolute values with respect to Fig. 5. 3 is not an effect of the polyethylene shielding of the photomultipliers alone, but mostly caused by the different radial range considered.

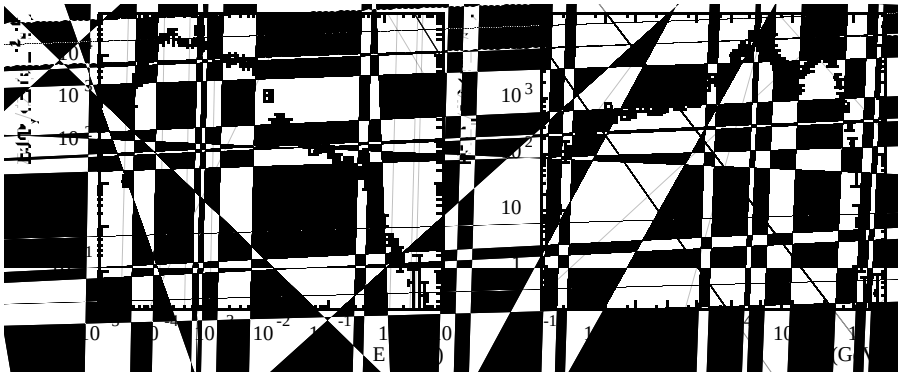

Fig. 5. 3: Energy spectra of photons (left) and neutrons (right) in the position of the photomultipliers. Values are for LHC peak luminosity.

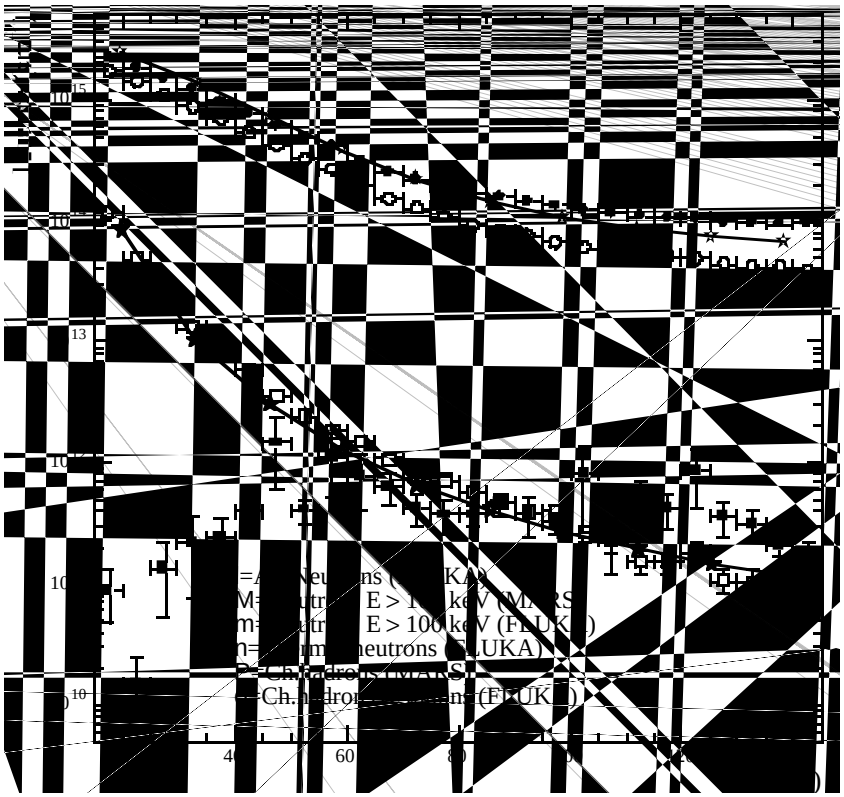

Fig. 5. 4: Fluence of different particle types just behind the absorber as a function of radius. Values are for $5 \times 10^5 pb^{-1}$. The muon contribution to the charged fluence, quoted for FLUKA, is only a few tenths of a percent so the pure charged hadron curve would be almost indistinguishable from the present one. The legend (top to bottom) refers to largest to smallest values.

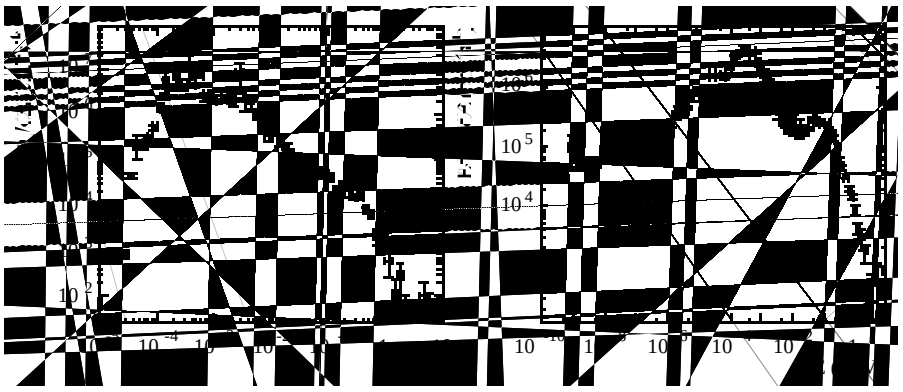

Fig. 5. 5: Energy spectra of photons (left) and neutrons (right) just behind the HF absorber averaged over radii *r*=20 cm to *r*=60 cm. Values are for LHC peak luminosity.

One important issue is where to place the electronics racks needed by the HF. Since the cable length from the photomultipliers to these racks has to be minimised, the most suitable position is just outside the lateral shielding of the HF. Fig. 5. 6 shows the fluence of different particle types in this position as a function of the longitudinal (z) coordinate. The large increase of fluence at z = 1080 cm is caused by the 3 cm wide crack between the endcap and the HF shielding. An inspection of the curves shows that most of the bulk damage in silicon devices will be caused by neutrons with energies above 100 keV. The contribution by other hadrons is relatively small.

Radiation dose is probably the more important parameter for the electronics racks. The dose as a function of z is shown in Fig. 5. 7. The dose just inside the borated polyethylene shielding is shown alongside the dose in the air just outside the shielding. As expected the dose in the polyethylene is higher, which can be attributed to recoils from *(n,p)* reactions. The dose in silicon itself should be close to that in air. In the rack, we can expect a certain amount of cables and other plastic items to accompany the silicon devices. Therefore, the two values should provide a proper estimate of the uncertainty in dose due to the material composition of the racks.

Both the fluence and dose have a soft minimum between z = 12 m and z = 12.5 m which thus is the preferred position for the racks. Beyond z = 13 m we observe a clear increase of fluences and dose, which is caused by the end of the absorber and therefore significantly reduced lateral shielding.

Fig. 5. 8 shows the energy spectra of photons and neutrons on top of the lateral shielding of the HF. While nothing unusual can be observed in the photon spectrum, the neutron spectrum is remarkably hard. The deficiency of thermal neutrons is explained by the borated polyethylene which forms the top part of the shielding. The fact that the 1 MeV evaporation peak has almost disappeared tells us that the shielding provides a very efficient neutron attenuation in the energy range where hydrogen is effective. The neutrons at about 100 MeV cannot be stopped, except with very massive shielding for which we have neither the space nor the possibility of support.

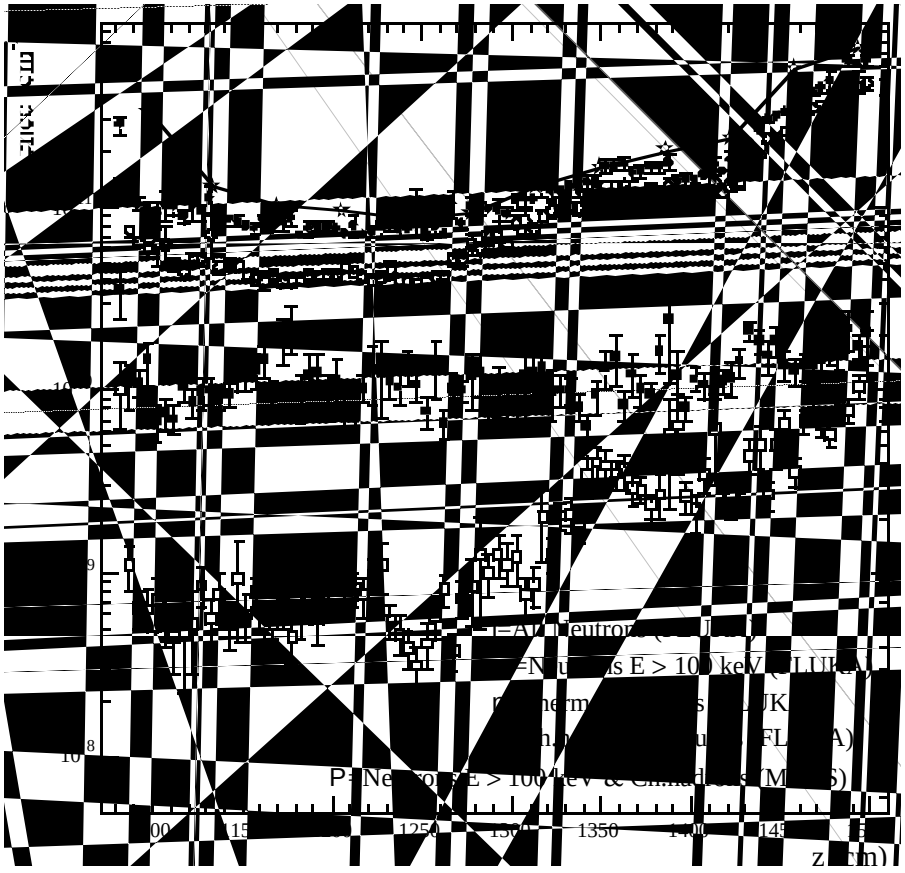

Fig. 5. 6: Fluence of different particles around the HF lateral shielding as a function of z-coordinate. Values are for 5×10^{5} pb^{-1}. The legend (top to bottom) refers to largest to smallest values.

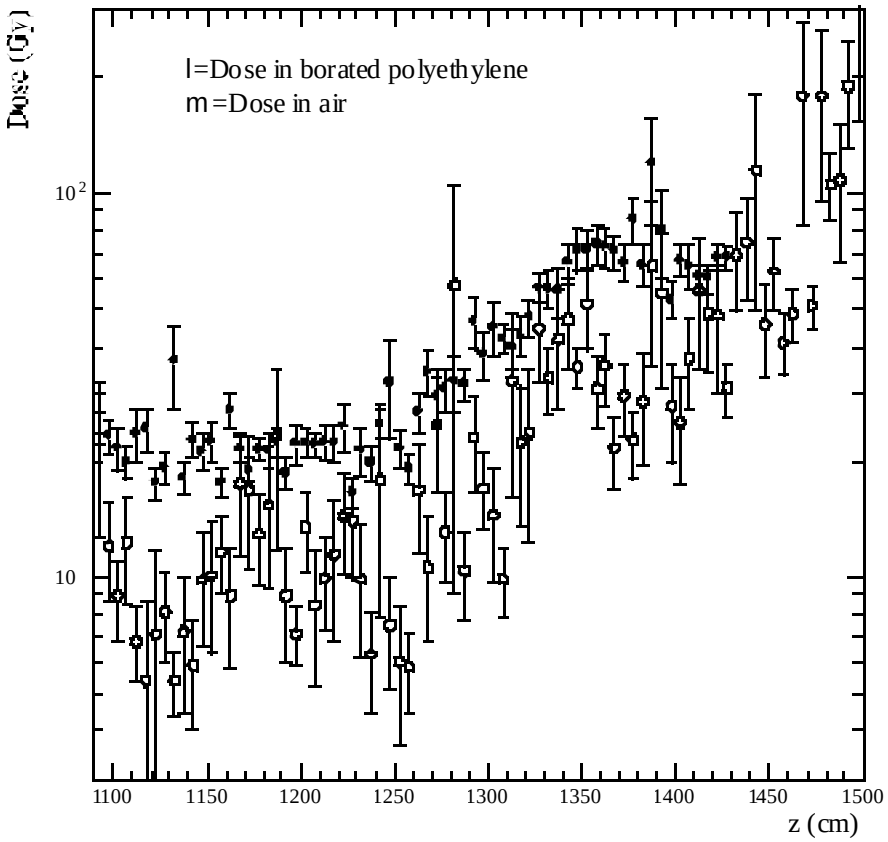

Fig. 5. 7: Radiation dose around the lateral shielding of the HF as a function of *z*-coordinate. The large error bars in the air values are caused by the low density, which reduces the number of energy deposition events. Values are for 5×10^5 pb^{-1}. The legend (top to bottom) refers to largest to smallest values.

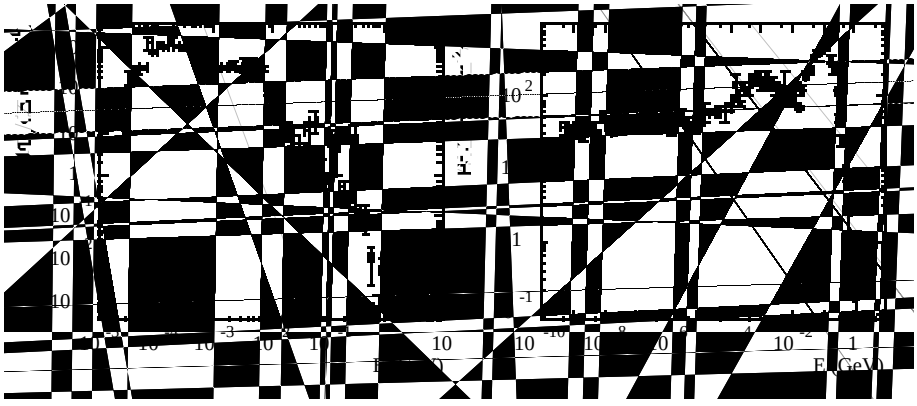

Fig. 5. 8: Energy spectra photons (left) and neutrons (right) around the HF lateral shielding where electronics racks are positioned. Values are for LHC peak luminosity.

5.3 TRANSPORTER PLATFORM

The transporter platform is designed to fulfill the following functions and meet the listed requirements:

a) transportation of the HF between the garage position and the foot of the elevation system;
b) adequate strength in supporting the weight of the HF and its shielding elements (~310 tonnes) as it is raised/lowered to/from beam position;
c) 25 cm motion on the horizontal plane for each half of the HF to facilitate installation of the HF around the beam pipe and eventual maintenance of the HF itself when in the garage position;
d) 30 cm motion along beam direction when the HF is raised to the beam height to ease installation of the detector between the endcap muon system and the rotating shield arms;
e) sufficient surface for the installation of the HF endplug shielding and 40 cm shielding collar between the HF shielding and the rotating shielding;
f) mechanical interface elements between the hydraulic jacks and support frames;
g) rolling mechanism that is consistent with the construction, assembly and installation plans of the HF detector;
h) mechanical structure that conforms to the radiation shielding requirements;
i) alignment system that is integrated to the HF detector system and the rest of the experiment.

The details of the transporter table are shown in Fig. 5.9 through Fig. 5.12. Fig. 5.9 shows half of HF positioned on the transporter platform. The transporter platform is equipped with four airpad feet at each corner. This type of airpad is also used for the CMS magnet elements and has been successfully tested recently. Fig. 5.10 illustrates the details of the horizontal motion of the detector on the platform. A pair of channels is located on top of the table to guide the rollers that are shown in Fig. 5.11. The motion along the beam direction is accomplished in a similar manner along the channels at the bottom of the table. Fig. 5.12 shows both side view details of the transporter table.

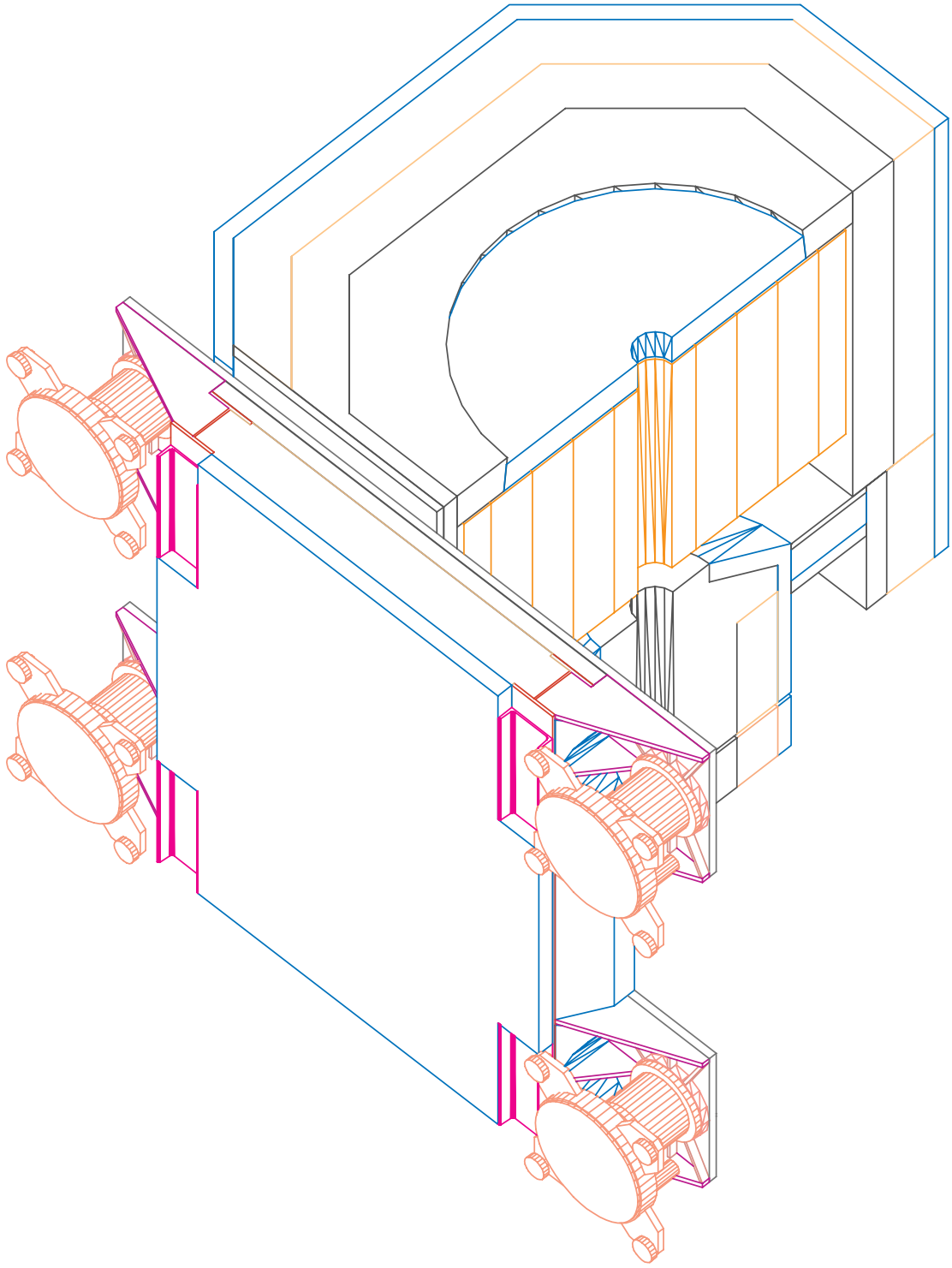

Fig. 5.9 (C.S.): The bottom view of the transporter table is shown above. The half of the HF detector and the endplug shielding are positioned on the table. The motion of the table is accomplished by four airpad feet located at its corners.

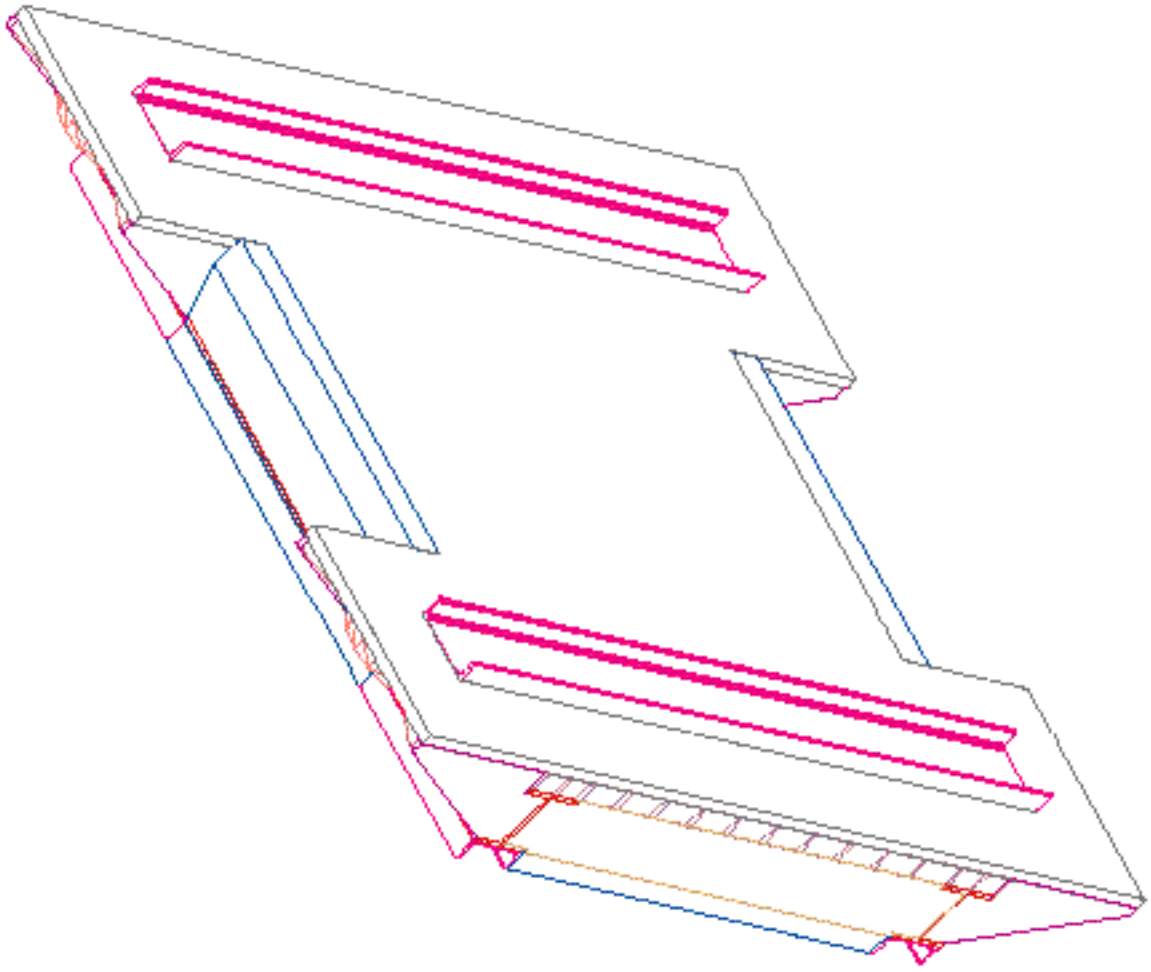

Fig. 5.10 (C. S.): The top view of the transporter table shows the channels for the horizontal motions; left and right movement of each detector half (channels located on top of the table) and the motion along the beamline (channels positioned at the bottom of the table).

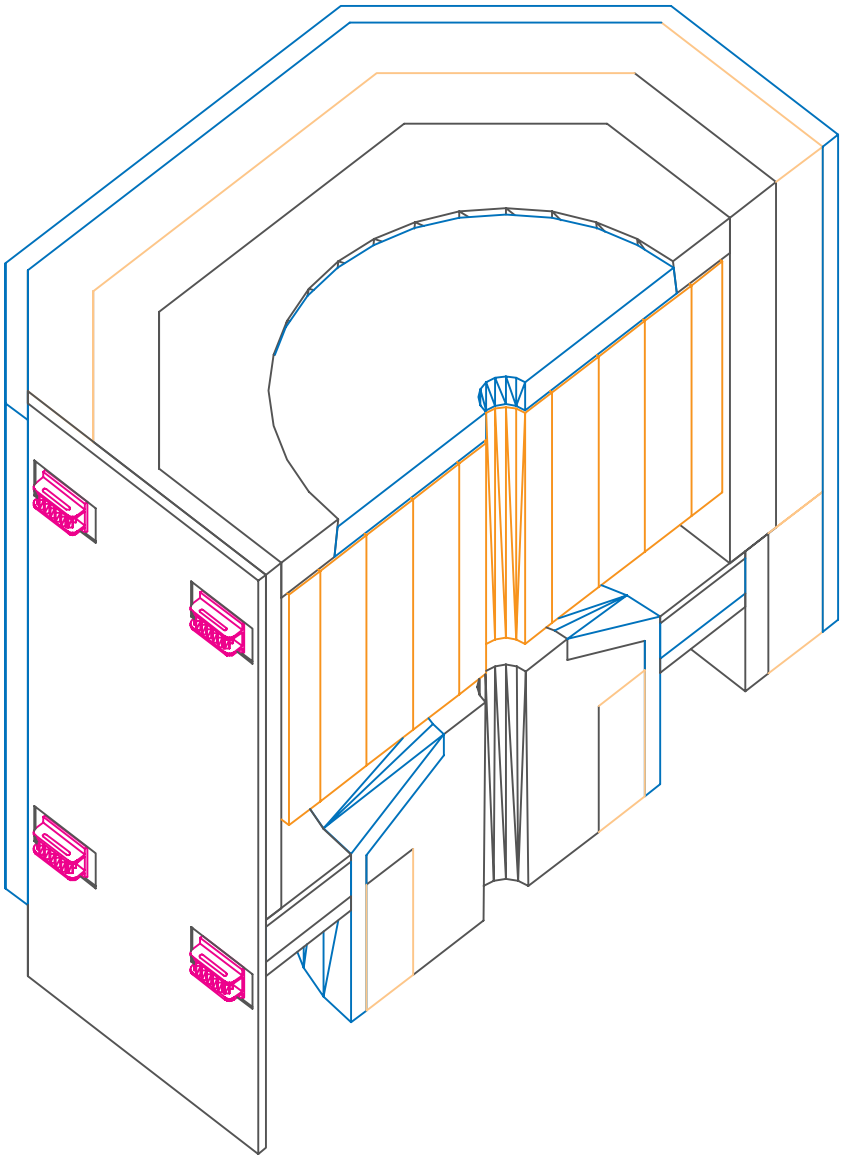

Fig. 5.11 (C. S.): Four heavy-duty rollers are located at the bottom of each detector half. These rollers move along the channels for left/right motion and also used in the assembly sequence.

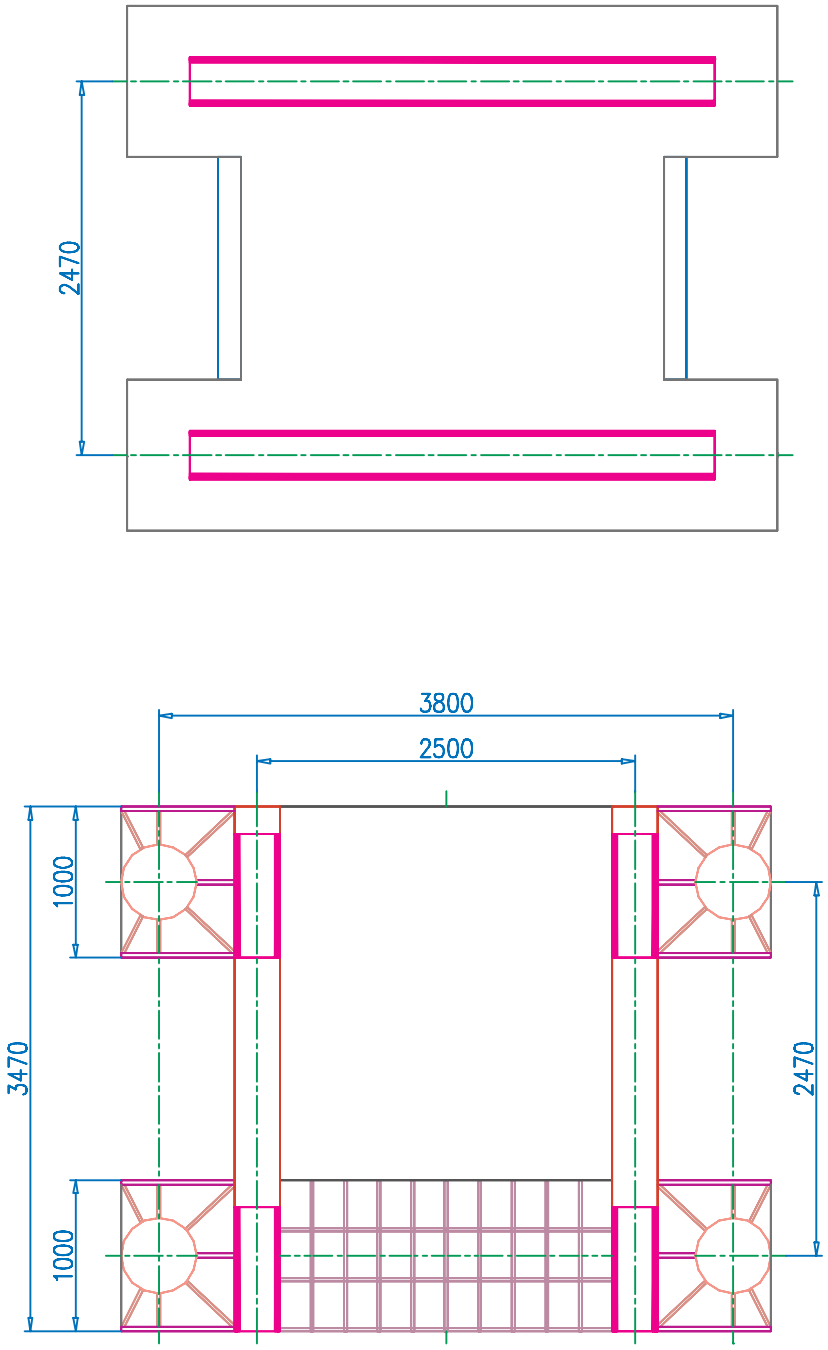

Fig. 5.12 (C. S.): The details of the transporter platform are illustrated above. The top drawing shows the top view and the bottom sketch illustrates the details of the airpad locations and the channels that assist in the z-motion.

5.4 HF ELEVATION SYSTEM

The beamline is ~8.6 meters above the floor level in the experimental area. The forward calorimeters need to be elevated and secured in position before data taking commences. Since the HF detectors are located outside of the main body of CMS, they will be installed into the beam position towards the end of the entire CMS assembly sequence. If access to the inner components of CMS is required during a shutdown, at least one of the HF detectors needs to be

lowered and put in garage position. In order to make installation and deinstallation of the HF possible, an elevation system is designed as shown in Fig. 5.13. This system is required to handle the entire weight of HF including its shielding (310 tonnes), and to vertically position the detector within ± 1 mm of the beam center.

A set of four hydraulic jacks is located under the floor surface to raise the detector with the transporter table. Fig. 5.14 shows the locations at the corners of the platform where the jacks are located. This is the same location as the airpads. The detector is raised and a frame is slid under it. The frame would support the table on the flats shown at four corners. The rollers for the motion along the beam line are located just above these flats. The lifting flaps that are attached to the columns of the frames are used to further elevate the detector as shown in Fig. 5.13.

The raising and lowering operations will have to be performed by a team of crane and rigging operators. It is expected that it would take about a day to position the HF in the beam. A 10 cm thick lead shielding element is planned to be located in the front part of the HF during these operations to reduce the radiation background originating from the HF absorber. Further studies are underway to understand the nature of the activation radiation to facilitate optimal shielding.

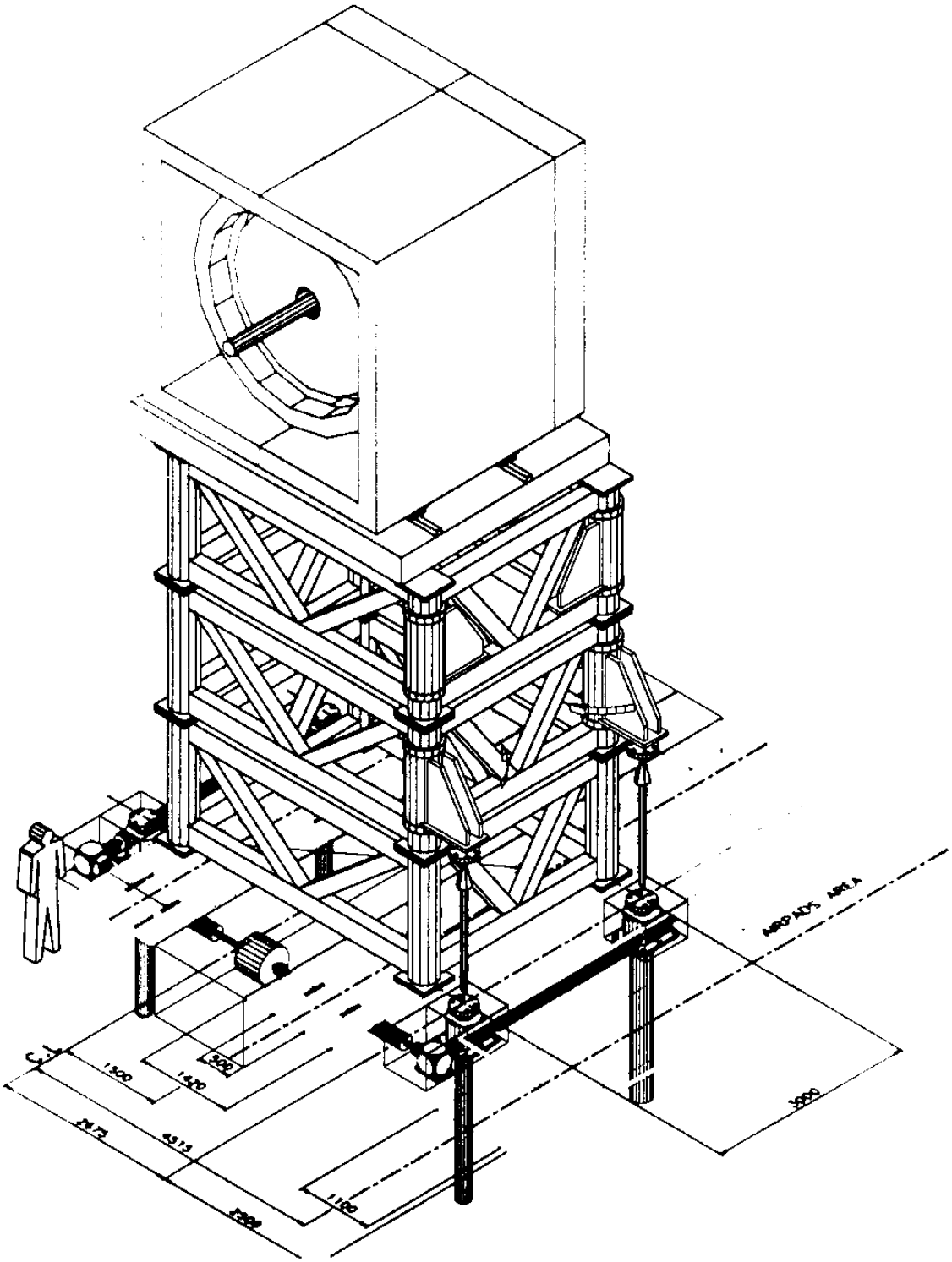

Fig. 5.13: The elevation system is shown above where three frames are used to support the weight of the HF and its shielding. The HF and the transporter platform are shown schematically.

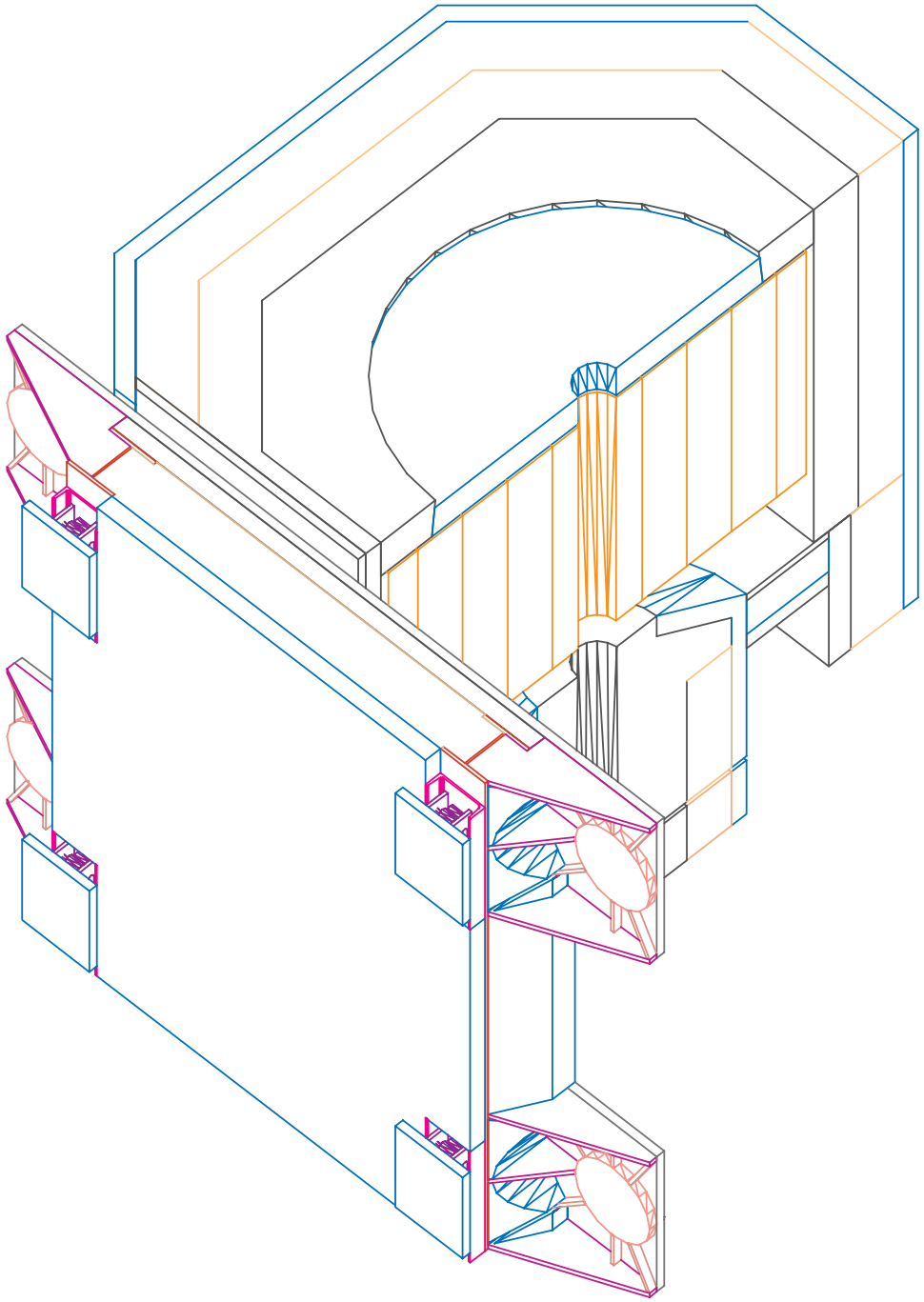

Fig. 5.14: Bottom view of the HF and the transporter table. Note that the airpads are removed and the four flats are shown where the upright columns of support frames mate the platform.

5.5 HF GARAGE POSITION

The HF garage is designed to meet multiple requirements and provide flexibility in HF manipulation and maintenance in general. A layout of the garage is shown in Fig. 5.15.

a) During the assembly and installation phase of CMS, the HF can be located away from the usable floor space of the experimental hall in the garage. This provides room for the endcap

systems (muon chambers and calorimeter) to be fully retracted out of the barrel, e.g. for tracker installation in the beginning and later, for other maintenance needs.

b) HF PMT and electronics installation, testing and maintenance activities can be carried out in the garage position without interference with any other CMS subsystem.
c) The garage dimensions are 6.1 m high, 7.3 m deep and 7.1 m wide. The optimization of the transporter platform design, commensurate with the shielding requirements, provided minimization of the total height of the detector. This makes installation of a crane in the garage possible. The width of the garage is sufficient to open the two halves of HF by almost a meter apart for maintenance. The depth provides ample floor space for storage of spare modules, shielding elements and other equipment.
d) The entrance door to the garage from the side walls is at elevation of three meters which makes access to the upper electronics racks rather convenient. A walkway at this elevation is foreseen towards the back of the garage.
e) A 5-tonne crane is planned for the garage. This would enable us to manipulate the absorber modules (2.7 tonne max) and other shielding elements if it proves necessary.
f) A temporary lead shielding against the radioactivated HF absorber will be in place when the detector is in motion between the garage and the data taking position as pointed out earlier. In addition, when the detector is in its garage position, the sliding doors of the garage (15 cm concrete with a 5 cm thick lead insertion with a radius of 50 cm centered around the HF symmetry axis) will provide additional and adequate shielding.

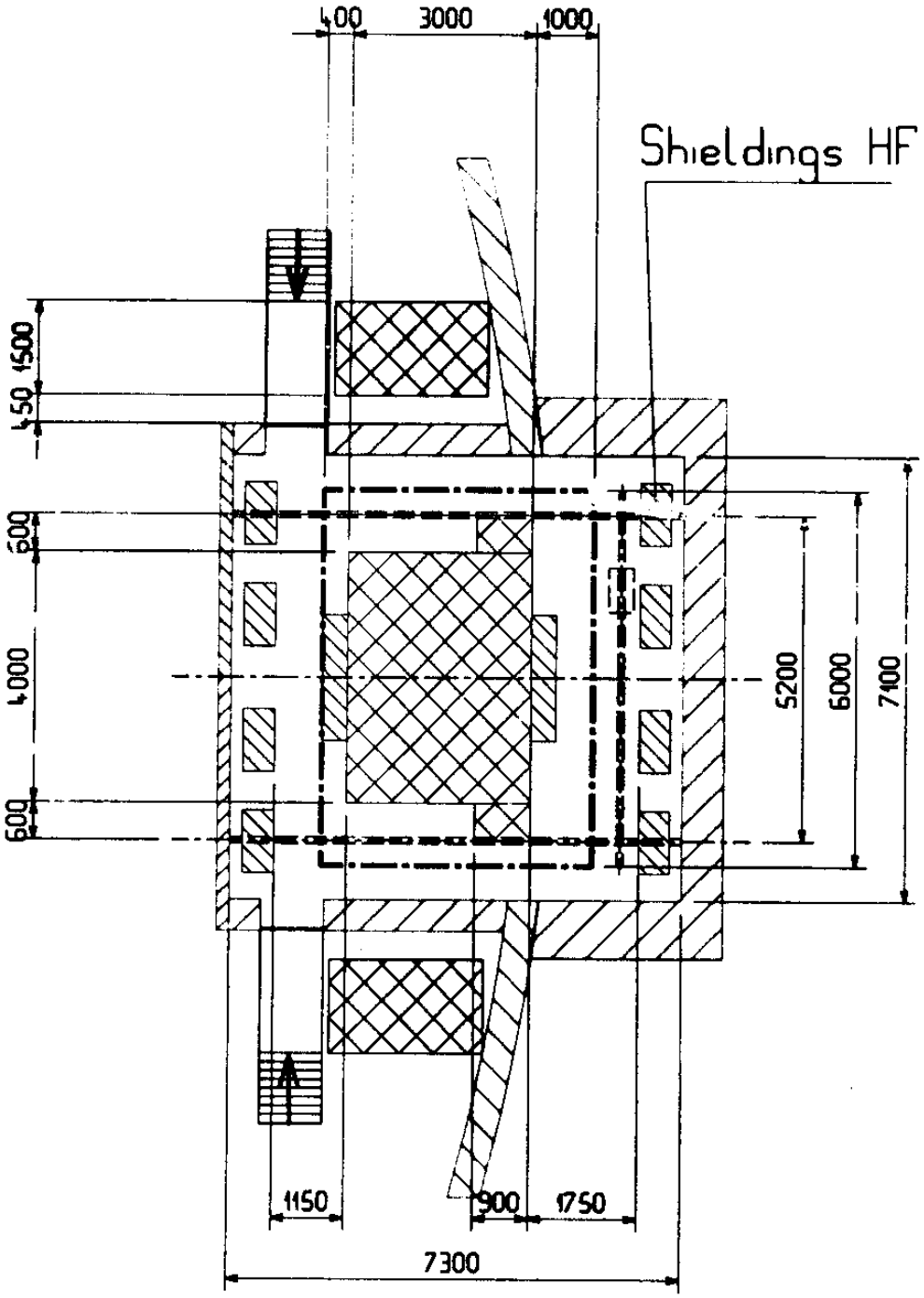

Fig. 5.15: The layout of the HF garage (top view).

5.6 FORWARD CALORIMETER DESIGN

5.6.1 Overview, constraints, specifications and requirements

The main requirements for the HF are the following:

a) Phase space to be covered by the HF spans η=3 to 5 which is 40% of the available phase space of CMS. HF covers this region with good hermeticity, fine transverse granularity, adequate energy resolution and a sufficient depth. At z=±11.1 m, where the front face of the HF is located, the active radius is 1.40 m with a depth of 1.65 m or 10 nuclear interaction lengths, λ. The tower structure is chosen to be in a square geometry; for $|\eta|>4$, the towers are 5 cm×5 cm, and for $|\eta|<4$, towers are larger, 10 cm by 10 cm square (see Fig. 5.16). The dead-zones are kept to absolute minimum in order not to adversely affect the missing energy measurement.

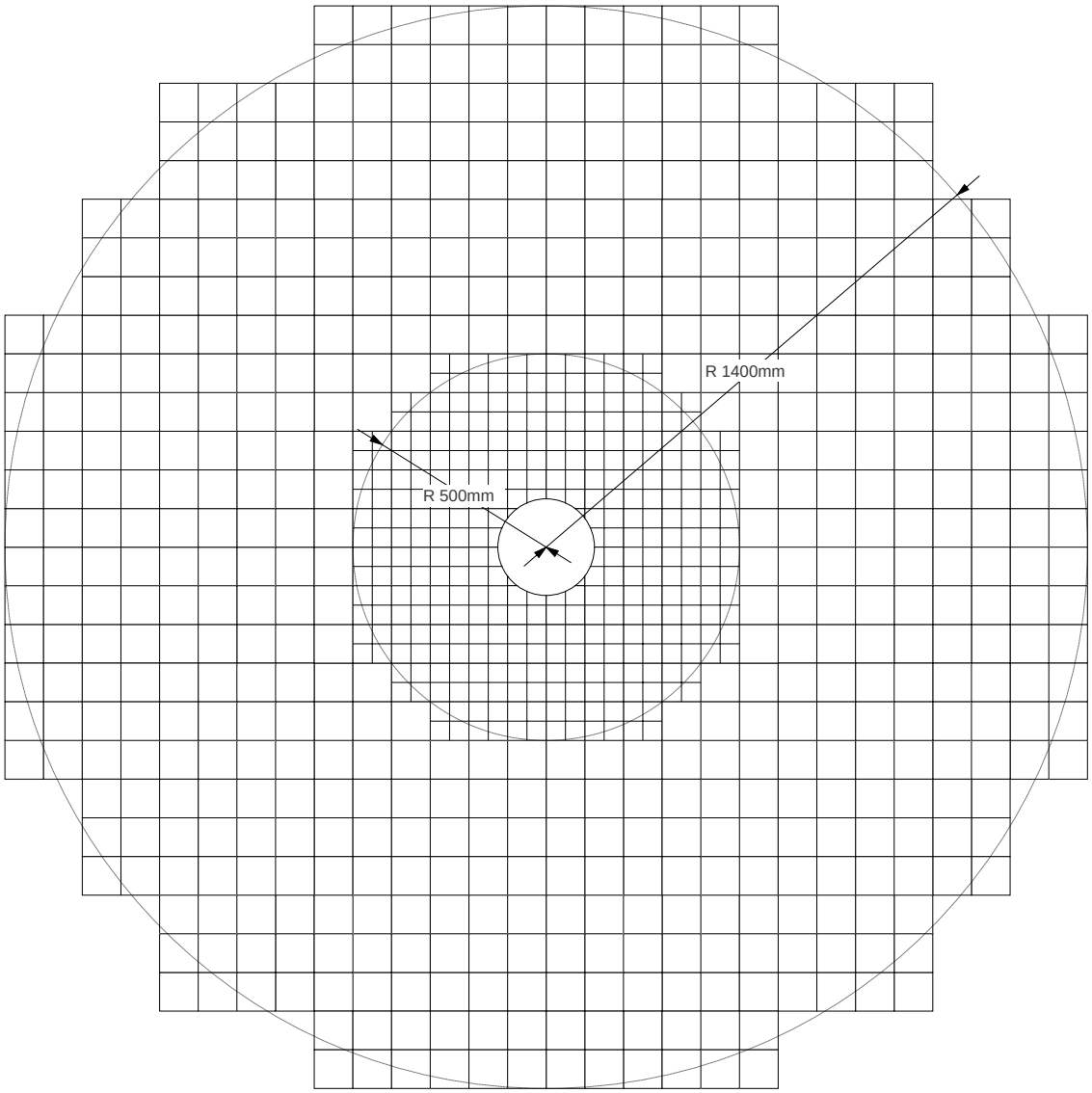

Fig. 5.16: The HF front face is shown with the tower structure as described in the text. The smaller (5 cm×5 cm) are closer to the beam pipe region and the coarser towers are located at η<4. The inner radius is 12.5 cm.

b) The HF must maintain its intended functionality even at the exceptionally high levels of radiation expected at LHC. The radiation doses of up to a Grad over ten years are anticipated in the hottest region of the HF. The choice of quartz as the active medium serves this purpose well since it can withstand doses up to 30 Grad with only a few percent loss in

transparency in the wavelength range of 300-425 nm[2].The accumulated dose from all sources and types of radiation at the PMT location does not exceed 10 krad/year, and at the electronics racks that are located outside the shielding elements, the total dose per year is about 3 krad. These doses are acceptable for satisfactory detector performance. Extensive radiation background studies resulted in the shielding configuration shown in Fig. 5.17.

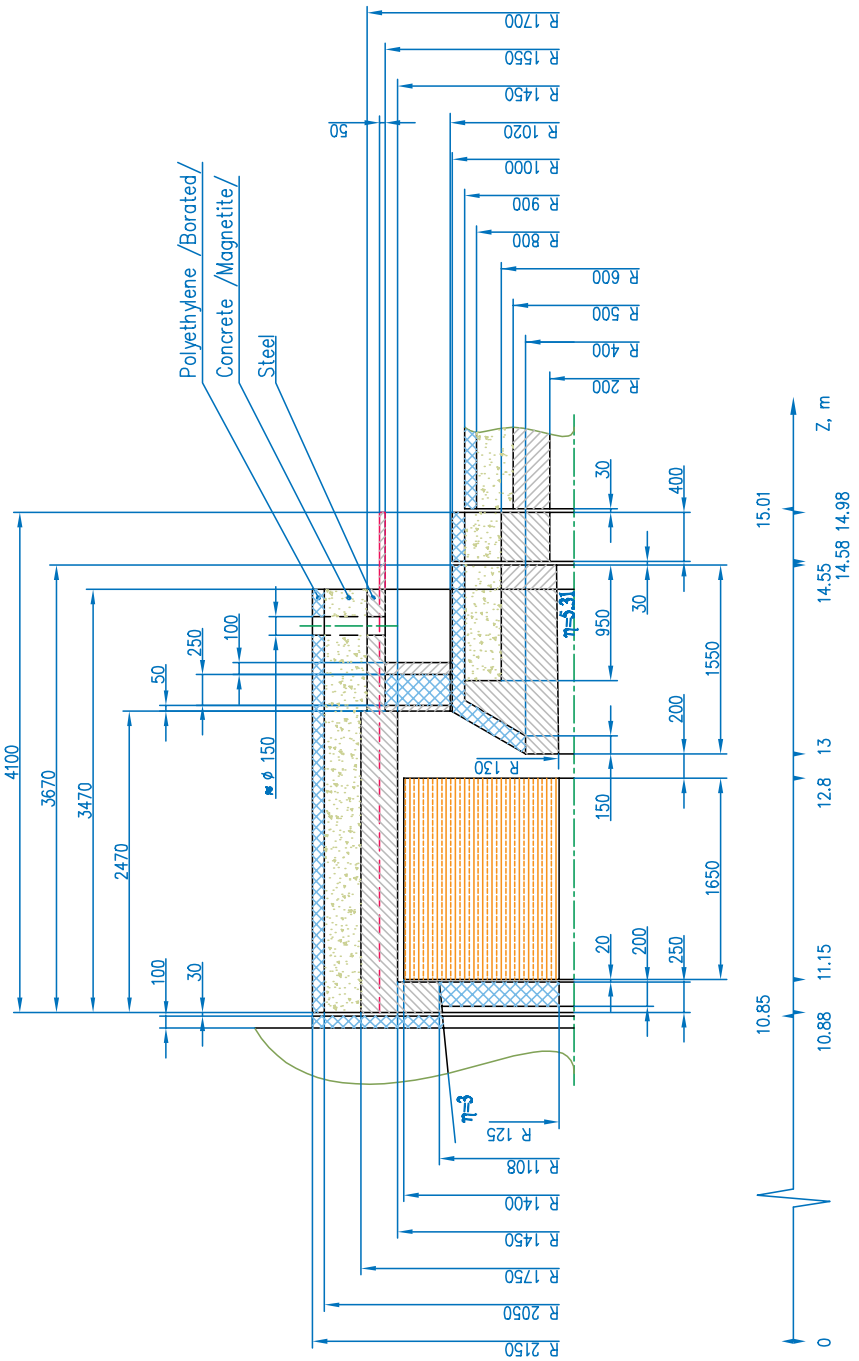

Fig. 5.17 (C. S.): The HF is surrounded effectively by 30 cm thick steel, 30 cm thick magnetite concrete and 10 cm thick borated polyethylene. In front, the HF is covered by a 20 cm thick polyethylene, and in the back, a plug structure shields the PMTs and fibre bundles. PMTs are located around a ring at 100 cm<*r* <140 cm.

c) The neutron rates in the vicinity of this detector will be exceptionally high. One of the fundamental features of this kind of a detector is that neutrons do not produce Cherenkov light and therefore do not contribute to noise in the detector. The total neutron fluence immediately behind the copper absorber and closest to the beam pipe, for 5×10^5 pb^{-1}, is about 2×10^{15} n/cm^2. The fibre bundles will be located in this region. 140 cm away from the beam, the neutron fluence drops by an order of magnitude. The PMTs are well shielded behind a 40 cm thick matrix of steel and borated polyethylene slabs against the radiation emerging from the absorber region. Thus, the neutron fluence here is reduced to ~ 2×10^{12} n/cm^2 for 5×10^5 pb^{-1}. The HF PMT window will be made of silica glass with superior radiation resistance properties. No appreciable transmittence loss is observed up to a total dose of 1.4×10^{14} neutrons/cm^2 in the wavelength range of operation with these types of window materials.

d) The HF is being designed such that it integrates well with the rest of the CMS subsystems. These subsystems are:
   - Endcap Muon System: The ME4/HF interface region is redesigned based on the results of the radiation background simulation results. The general difficulty has been to isolate the higher η regions of the ME4 muon systems from high neutron rates that originated from the HF and other sources. This problem is solved to a large extend by introducing a 25 cm thick steel and a 10 cm thick borated polyethylene in this interface region. The steel section is part of the HF shielding and radially covers from r = 110.8 cm to r=175.0 cm. A 10 cm thick polyethylene slab is attached to the backplane of ME systems such that it conforms to the HF projection onto the back of the muon system. This slab radially covers from r =110.8 cm to r=215.0 cm. A 3 cm air gap is foreseen in this region to facilitate the z-motion of HF when being installed/deinstalled in the beam position. In addition, a 20 cm polyethylene shielding is located in the front face of HF to reduce the backsplash albedo.
   - Beam pipe and the vacuum pumps: A straight 20 cm diameter stainless steel beam pipe goes through HF. The thickness of the beampipe is about 1.5 mm. The current design of beam pipe calls for a change from 6 cm radius to 10 cm. This makes relocation or perhaps complete elimination of the vacuum pump in front of the HF possible. Further studies are presently carried out to simulate the vacuum conditions at the IP. Although a conical pipe inside HF might seem desirable at first sight, the background simulations do not indicate an appreciable difference between these two geometries. The HF is designed to separate in two halves such that it can envelope the beam pipe when installed in its final position. The beam pipe will remain in position when HF is installed/deinstalled. The HF design respects 2 cm stay-clear beam pipe zone.
   - The rotating shielding: The rotating shielding is located in the back of the HF end-plug shielding. The rotating shield ends at z=14.96 m. A 40 cm long collar interfaces the rotating shielding with the back of the HF end-plug. This collar is the very last shielding element that is installed after the HF is positioned in its final beam position.
   - Transporter: The transporter consists of two fundamental elements; the table that HF is mounted upon and the elevation mechanism. The details of these systems are already outlined in sections 5.3 and 5.4, respectively. The transporter table is designed such that each half of HF is able to move by $\pm$25 cm on the horizontal plane and that 30 cm motion along the beam is also required for final positioning of the calorimeter. The HF is elevated to the beam height by hydraulic jacks and frames and positioning

tolerance of about ±1 mm is expected. The total weight of the detector is 310 tonnes, including the shielding. The beam center is 8.6 m above the floor level.

e) In the location of the PMTs, the magnetic field at most is a few hundred gauss. The shielding material combined with a 0.5 mm thick μ-metal is adequate for this purpose.

f) The trace elements in the composition of the absorber material (C110, 99.5% Cu), should not contain elements that are readily activated. One such element is Co and the typical levels in industry produced plates are low, 0.005 to 0.006%.

The HF is constructed such that there are three different lengths of fibres inserted into the absorber as illustrated in Fig. 5.18. The long fibres that run the entire length of the absorber (165 cm) are called *long* fibres. The *medium* length fibres are shorter by 22 cm (15 X_o) from the front face of HF. The *short* fibres are inserted 30 cm (2 λ) from the back face of HF. Consequently, *long* fibres constitute the electromagnetic (EM) section, *medium* fibres, the hadronic (HAD) section, and *short* fibres, the tail catcher (TC) sections.

Table 5. 2 summarises the HF tower structure parameters.

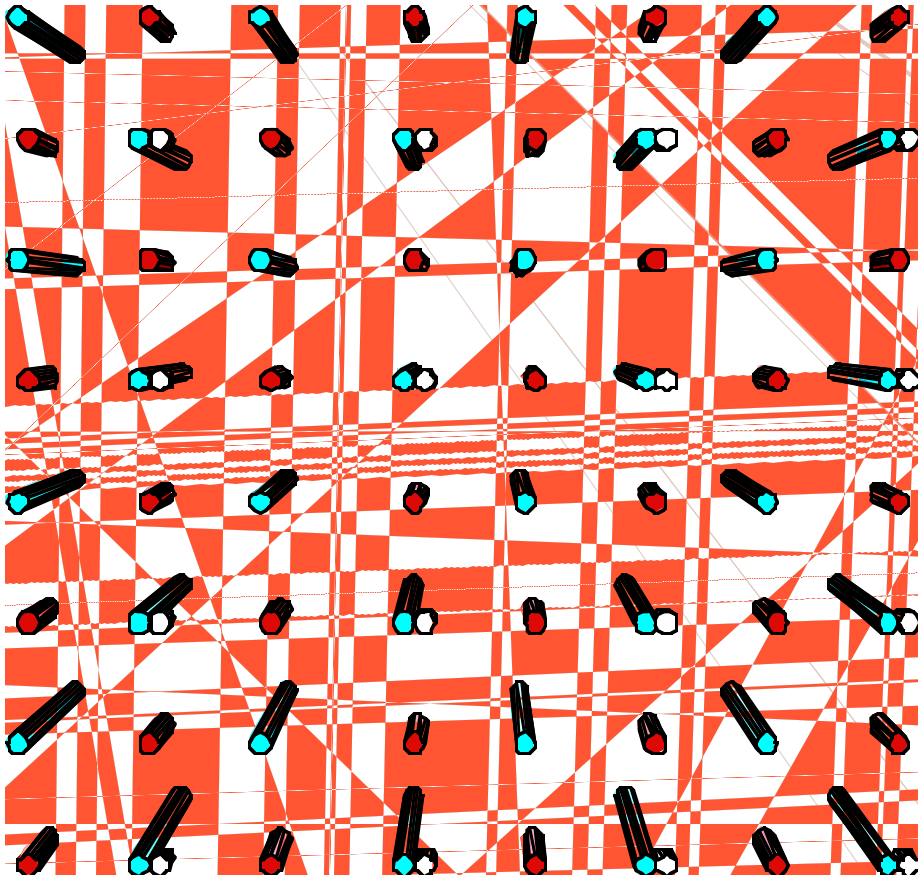

Fig. 5.18 (C. S.): Three different length fibres are located in the copper absorber in 2 mm square geometry. EM fibres that run the entire length of the absorber (165 cm) are schematically shown next to the TC fibres (inserted 30 cm into the absorber from the back of the calorimeter at every other plane) and the HAD fibres are shown as single fibres that are located at every other groove and plane and they are shorter by 22 cm with respect to the EM fibres.

Each section is readout by an individual photomultiplier. The tower structure is of square geometry. Close to the beam pipe ($\eta>4$) the tower size is 5 cm×5 cm square and everywhere else it is 10 cm×10 cm square as shown in Fig. 5.16.

Total HF depth is chosen to be ten interaction lengths, which is more than sufficient for the required physics performance. Increasing the absorber from eight to ten interaction lengths, a factor of two to three reduction is gained, on average, in all particle fluxes behind the calorimeter. A side view of the HF showing the shielding is given in Fig. 5.19.

Table 5. 2

The HF tower sizes and other parameters. The number in parentheses indicates the number of fibres for that tower.

Tower type	Size (cm × cm)	Quan./Side	EM Length (cm)	HAD Length (cm)	TC Length (cm)
Small ($\eta>4$)	5 × 5	320	165 (313)	143 (313)	
Large ($\eta<4$)	10 × 10	564	165 (1250)	143(1250)	
TC Tower	20 × 20	164			30 (2500)

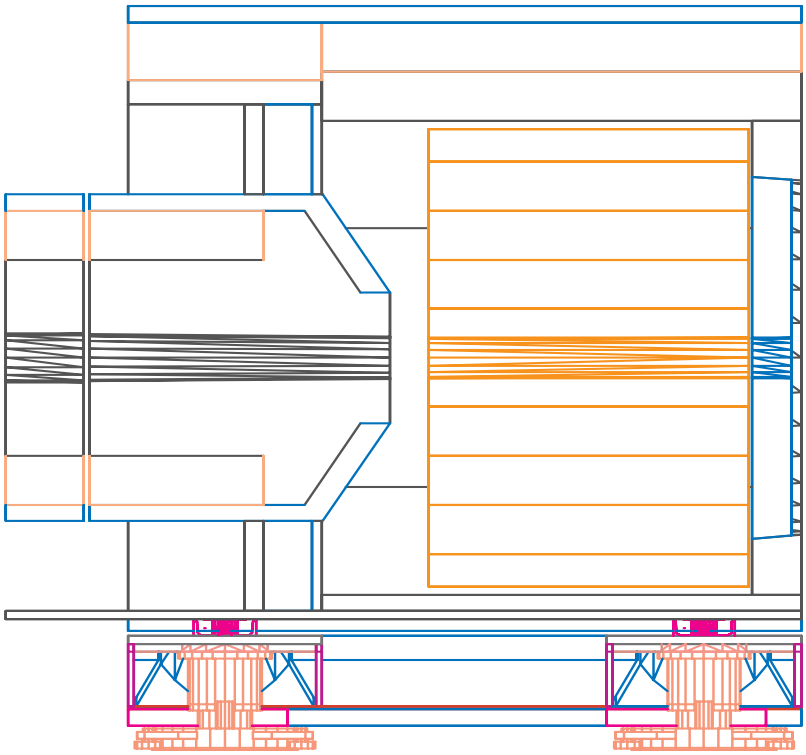

Fig. 5.19 (C. S.): The side view of the HF shows the absorber, the shielding end-plug and the transporter platform (IP on the right). The fibre bundles are arranged such that EM, HAD and TC fibres emerge in the back of the absorber and get connected to the right side of the back shielding (around the end-plug) via ferrules. PMTs are located to the left.

5.6.2 Absorber matrix

The basic construction element of the HF absorber is a module with holes for quartz fibres. The quartz fibres will laterally form a square matrix where the closest neighboring fibres are equidistant, 2 mm. Each hole will contain one (for EM section) or two (for HAD and TC sections) fibres of 345 micron diameter (including cladding and buffer thickness). Four different types of modules will be used in construction of the HF absorber. The main features of each of the module types are listed in Table 5.3.

Table 5. 3

Four different types of modules will be used in constructing the HF absorber. The main features of each of the module types are listed below.

Module Type	Size (w × h) (mm × mm)	Weight (tonne)	Quantity
I	600 × 300	2.66	32
II	500 × 300	2.22	32
III	300 × 300	1.33	16
IV	600 × 200	1.77	8

Modules will be made of copper plates with grooves. Plates will be stacked together using diffusion welding such that the modules will be self-supporting structures. The dimensions of the grooves are shown in Table 5.4.

Table 5. 4

Dimensions of grooves in the absorber plates.

Groove center-to-center (mm)	2.00 ± 0.10
Groove depth (mm)	0.5 + 0.2 - 0.1
Single groove width (mm)	0.5 + 0.2 - 0.1
Double groove width (mm)	0.9 + 0.2 -0.1

We have used photochemical etching to produce grooves in the copper plates of the prototypes. Our experience indicates that the required dimensions and tolerances can be achieved with this technique. The cold rolling seems more advantageous for mass production. Rolling technology is currently being refined for production of full size copper plates to the required groove dimensions and tolerances. This technique will be adapted for grooved plate production if it proves compatible with the construction procedures and requirements.

The module will be machined to size after the plates are welded. Top and bottom plates have allowance of 1±0.4 mm for achieving linear dimensional accuracy and surface flatness. After machining, the tolerances of ± 0.1 mm on the height and on the width is aimed for each block. The edges will be flat and parallel to within ± 0.1 mm. Dimensions and tolerences of the plates are given in Table 5.5 while modules are specified in Table 5.6.

The following inspections will be used for the quality control during the manufacturing cycle of the absorber modules:

a) inspection of copper plates -- dimensions and flatness of 5% of plates will be measured;
b) inspection of grooved plates -- dimensions of grooves for 5% of plates will be measured;
c) inspection of the welded modules -- the welding quality of each module will be tested at the vibration stand and with ultrasonic and/or X-ray techniques when appropriate. The dimensions of the holes will be checked using steel wire gauges.
d) inspection of machined modules -- outer dimensions and flatness will be measured using a rolling pass, the weight of the module will be measured to control the average density of the absorber.

Table 5. 5
Dimensions and tolerances of copper plates. The flatness tolerance is 0.1 mm and the edge -to-edge angle is 90˚ ± 1′.

Plate Type	Width (mm)	Thickness (mm)	Length (mm)	Quantity
I	602.0 ± 0.5	2.00 ± 0.20	1650 ± 0.5	5,600
II	502.0 ± 0.5	2.00 ± 0.20	1650 ± 0.5	4,800
III	302.0 ± 0.5	2.00 ± 0.20	1650 ± 0.5	1,200

Table 5. 6
The tolerances on the modules. The flatness is 0.1 mm, edge-to-edge angle is 90˚±3′, and parallelism is 0.1 mm.

Module Type	Width (mm)	Thickness (mm)	Length (mm)
I	600.0 - 0.5 + 0.0	300.0 - 0.1 + 0.0	1650 ± 0.5
II	500.0 - 0.5 + 0.0	300.0 - 0.1 + 0.0	1650 ± 0.5
III	300.0 - 0.5 + 0.0	300.0 - 0.1 + 0.0	1650 ± 0.5

The quadrant tolerances will be -0.5 mm for the width and the height. The flatness of the top, bottom and the side surfaces will be within 0.5 mm. The angle between the side and top/bottom surfaces will be within 3′. The flatness of the side surfaces of the half of the HF is within 1 mm. The parallelism of the side surfaces for the entire HF is 0.5 mm.

5.6.3 Structural elements

The HF calorimeters are built in quadrants. It is convenient to assemble in quadrants both in terms of mechanics and, later, in terms of transportation, testing in a test beam, lifting/lowering and the final assembly in the assembly area.

One quadrant consists of 11 absorber modules, as described in the previous section, and mounted on a steel shell which provides structural support. The steel shell is also a part of the radiation shielding when installed. Before the assembly of a quadrant, the quality control of the necessary modules will have been performed and appropriate selections and modifications, if necessary, of modules will have been made in order to conform to the required tolerances for a given quadrant. A schematic of a quadrant is shown in Fig. 5.20.

The quadrant structure will be assembled in layers starting with the outer modules, *i.e.* those closest to the steel support shell. Possible gaps between the last absorber module and the support shell will be compensated for by shims. Several passes may be required in order to level the top and side of the quadrant. The expected deviation from the plane on the top and the outer side does not exceed 0.5 mm.

Fastening of absorber modules relative to each other is still being investigated. The absorber modules are not allowed to move with respect to each other or to the support structure while quadrants are transported, or a half of the HF assembled, or when the HF moves in and out of the garage. Among the options that are currently being considered are attaching the modules to the side wall of the shell with thin steel belts or bolting them together (at the expense of sensitivity loss) or epoxied together. Modules are held together from the side and top with 2 cm steel plates which encase the entire absorber matrix except the back where the fibres emerge.

The steel shell also serves as support for the segments in the back of the quadrant where the PMTs are located. The part of the shell which extends beyond the back face of the absorber is a separate unit. It is a structure with multiple pieces. This is necessary because of the fact that fibre insertion requires room behind the absorber and the pieces are attached and put together as the fibre insertion gets completed. The distance between the back of the absorber and the first 5 cm steel slab is 50 cm. The shielding matrix consists of 25 cm of polyethylene sandwiched by two layers of steel (5 and 10 cm thick, on either side of the polyethylene block). This matrix functions as a shielding component protecting PMTs and the experimental hall from background. The air-core mixers inside the through holes transport the light from the fibre bundles to PMTs located on the other side of the segments. The rear steel layer also shields the PMT against the magnetic field.

The entire structure (absorber and its steel shell) has rollers mounted on both bottom and side walls, so that it can be moved during assembly and installed onto the transporter platform. This design allows for the quadrants to be rotated by 90° and moved to assemble half of the HF as discussed in the next section.

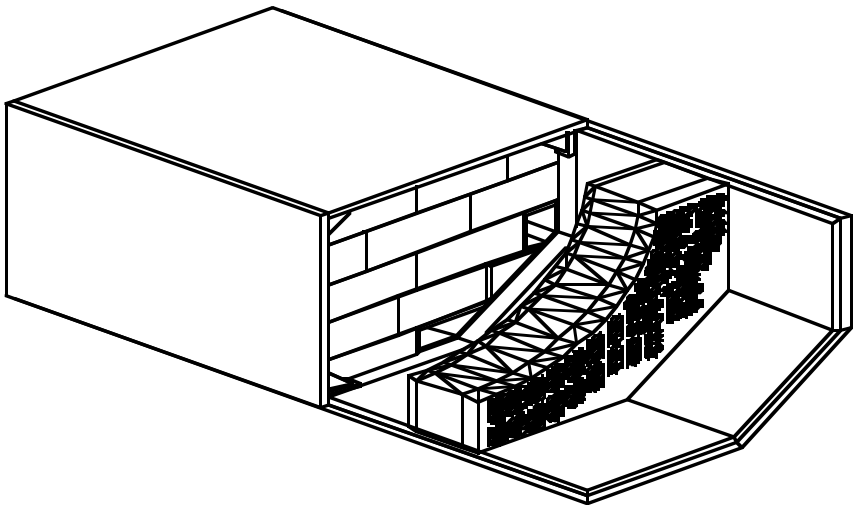

Fig. 5.20: One of the HF quadrants is shown schematically above. Steel plates cover the top and the side of the absorber. The back shielding and the through holes for the air-core light mixers are also indicated. The flanges that connect the back shell to the shell of the absorber can be seen around the inside periphery.

5.6.4 HF Assembly and installation

The HF and all of its shielding elements weigh 310 tonnes on the transporter platform. Naturally, assembly and installation of these massive components require adequate lifting and rigging capabilities. The construction, assembly and installation of these components need to be precisely planned in order not to exceed the limits of the existing cranes and other rigging equipment.

Static load due to the copper absorber alone per HF is 99.4 tons. The details are shown in Table 5.7. The detector must open in half to clear the beam pipe during installation. Thus, each half of the detector (~50 tonnes) must be structurally independent.

Table 5. 7

The static load due to the copper absorber per HF side is shown below.

Module Type	Weight/Module (tonnes)	Quantity/Side	Total (tonnes)
I	2.66	16	42.56
II	2.22	16	35.52
III	1.33	8	10.64
IV	1.77	4	7.08
TOTAL			99.4

Static load for shielding material is summarised in Table 5. 8 for each element. Note that each element is a sandwich of steel.

Table 5. 8

The static load due to the shielding elements per HF side is shown below.

Shielding Component	Weight/Block (tonnes)	Quantity/Side	Total (tonnes)
Top	9	2	18
Top-side	9	2	18
Side	15	2	30
Side-bottom	9	2	18
Platform+shielding	10	2	20
Endplug	5	2	10
TOTAL			114

The dynamic loads are small when the HF is in motion to and from the garage position. HF will be moved at a speed of ~ 5 mm/sec.

The installation plan calls for lowering the HF+ through the main shaft (PX56 with a 20.4 m diameter) when the 2500 tonne gantry becomes available in early 2003. This minimises the time spent on the experimental floor for assembly and shortens the general CMS assembly

and installation schedule. The effective dimensions of the smaller shaft (PM54) are 3.8×7.2 m^2 do not readily accommodate the entire HF on the transporter platform. We expect that at least one of the HF calorimeters (HF+) should be assembled/installed before other subsystems of CMS in the collision hall, *i.e.* YE/+3, +2, +1 and muon system.

A schematic illustration of the assembly plan is shown in Fig. 5.21 with steps (a) through (h) indicated. The absorber matrix (11 modules) and support structure are shipped to the assembly area (Building 168) in eight quadrants (a), each with mounted rollers on the bottom and side of the steel shell. Quadrants are rotated by 90° when a half of the HF+ or HF- needs to be put together. By this time, each quadrant has already been tested in a test beam and calibrated. Two quadrants are positioned relative to each other, and connected with two cm thick steel plates in the front and back.(b). The rear plate is auxiliary and can be removed as soon as the calorimeter is set into position on the transporter in the experimental hall. The half of the HF is rotated into vertical position (d) and, with the aid of rollers moved upon the transporter platform (e). The remaining half is also rigged on top of the platform at this stage as well (f). The shielding components are assembly tested (g and h).

All the steps shown in Fig. 5.21 are performed in the assembly area (Building 168). The shielding components after the assembly tests may be removed for transportation and lowering into the experimental all.

If either the HF construction schedule or the CMS general assembly is rescheduled, the lowering of HF into the experimental hall will be altered. There is a 80 tonne crane limit over the main shaft (PX56) which would require that HF be installed in pieces to the collision hall floor.

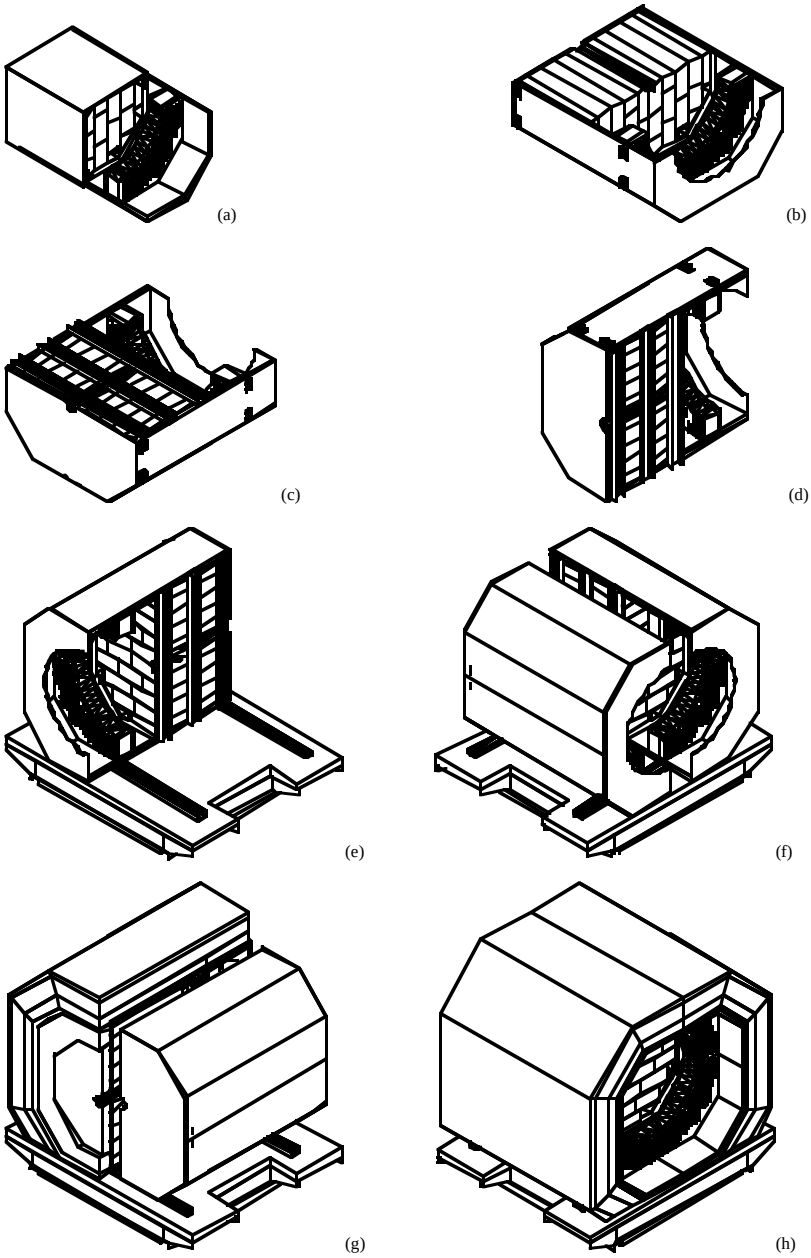

Fig. 5.21: The schematic illustration of the HF assembly is shown above.

5.6.5 Fibre layout

The fibre bundles that emerge from the back of the absorber are bundled into ferrules in order to couple to PMTs. The ferrules are connected to the 5 cm thick steel plate which is located in a ring structure between r =100 cm and r =140 cm. This connection is made using a pressure fitting. A conical hole is drilled into the steel plate and a slotted thin fitting over the cylindrical steel ferrule provides the necessary pressure to fix the bundle in place. The advantage of such a system is that the bundles do not need to be twisted during assembly and this mechanism provides sufficient strength, in addition to quick mount and dismount. We have tested this type of fittings up to 30 kg of force without failure. The expected force on the ferrules do not exceed a few kg.

Fig. 5.22 shows the coupling between the ferrule, steel plate and the light guides that

transport light to the PMTs. 5 cm steel plate holds the ferrules. This piece will be made in sections to make room available for fibre insertion work. As the fibre bundle are made, they are attached and secured to the steel ring. The ferrules are stainless steel cylindrical tubes, 7 cm long with an outer diameter of 2.5 cm. The inside diameters of the ferrules are different for smaller and larger bundles, corresponding to the tower sizes. The largest ferrule ID is about 1.9 cm which holds the 2500 fibres for the tail catcher towers. The ferrules will penetrate through the steel plate into the borated polyethylene by one cm. A hexagonal cross-section air-core light guide is positioned inside this 25 cm thick shielding element to transport the light from the end of the ferrules to the PMTs. PMTs mounted on PMT boxes are located at the outer side of the second shielding (10 cm thick steel slab) and mate with the light mixer via plastic fitting washer.

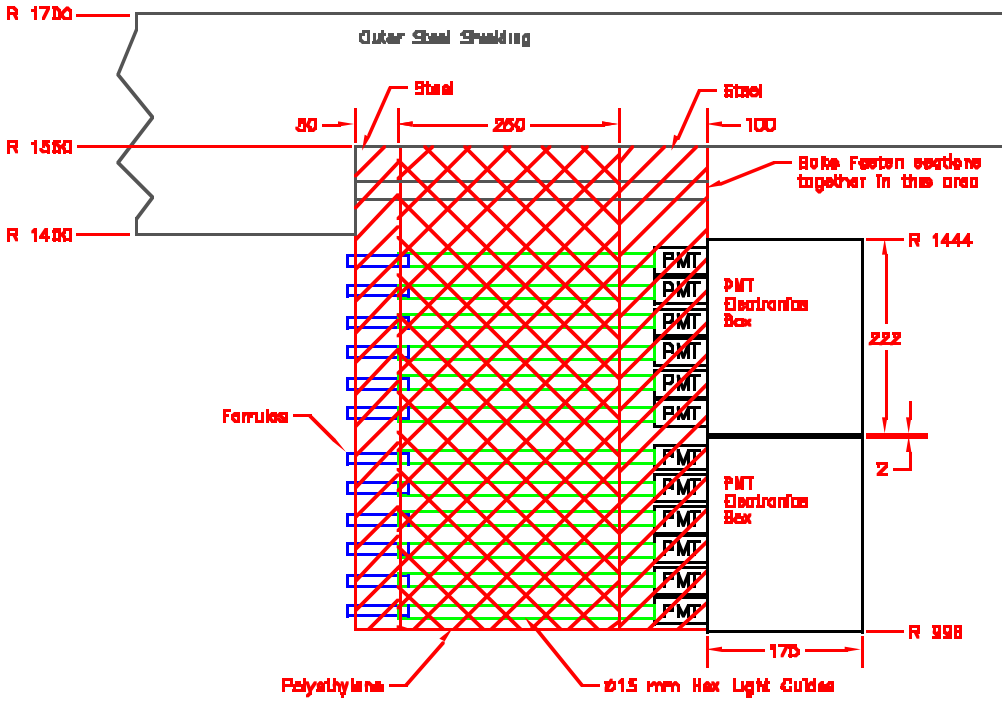

Fig. 5.22 (C. S.): The ferrules are coupled to steel plate via fittings as described in the text and light is transported through air-core light mixers to the PMTs located at the outer side of the second steel shielding slab.

There are 32 PMT boxes per quadrant as shown in Fig. 5.23. There are 16 PMTs mounted inside each box along with the calibration and monitoring components (laser and LED light distribution system and an input fibre for the quartz fibre radiation damage monitoring). The PMT boxes are located radially around the beam line between 100 and 140 cm and are geometrically arranged such that the quartz fibre bundle lengths from the towers are minimised and the available space is efficiently utilised. Each PMT box is identical and is mounted to the back of the steel shielding plane with the use of two quick release positioning screws. There is a 6 mm clearance space between the PMT boxes.

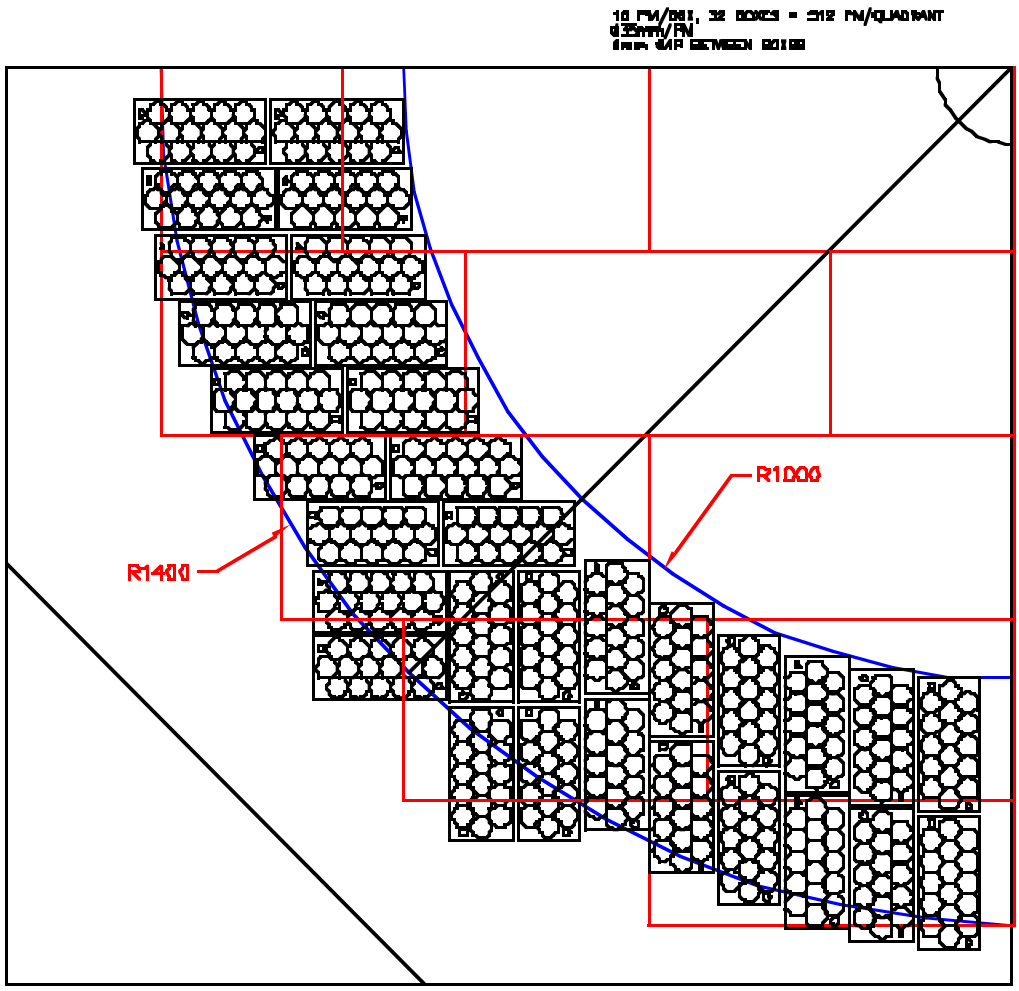

Fig. 5.23: The PMT boxes are arranged such that 512 PMTs are available per quadrant. Each PMT box is constructed identically and they are mounted to the back of the steel slab with the aid of two quick release screws for ease in installation and maintenance.

5.6.6 Photomultiplier layout/mechanics

The photomultipliers couple to the fibre bundles via air-core light mixers as described in the previous section. The PMTs are housed in a box as shown in Fig. 5.24. There are 16 PMT/box. Two quick-release screws attach the PMT box to the steel plate. Each PMT box is identical, and in addition to the PMTs, it houses the calibration and monitoring, Cockcroft-Walton high voltage components and nitrogen gas fittings.

The effective photocathode area of the PMT (dia 15 mm min) defines the dimensions of the light mixer and the fittings around the PMT head. A 0.5 mm thick μ-metal and a soft iron cylindrical housing extend 2 cm over the PMT photocathode (>2r) for magnetic field shielding. The soft iron housing is tapped outside at one end to be screwed into the faceplate of the PMT box. This minimises machining and cost while providing flexibility. Between the soft iron housing and the μ-metal shielding, a helical coil serves as a spacer and centers the PMT along the symmetry axis. This arrangement also allows the nitrogen to flow from the box volume towards the PMT head.

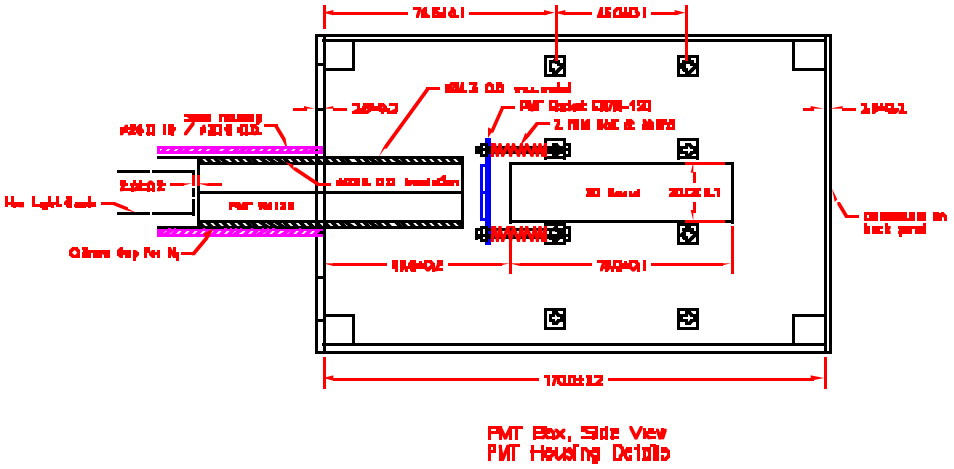

Fig. 5.24: The PMT and the PMT box cross section are shown above with mechanical details. The PMTs penetrate into the steel shielding by 4 cm. Connectors for signals and nitrogen are mounted on the back panel of the box.

Nitrogen is used to keep the He levels as low as possible around the PMTs since He permeability of silica glass window is higher compared to other standard glasses. This also protects the PMTs from catastrophic loss due to a possible He leak in the experimental area from cryogenic systems.

The PMT is connected via a socket to the circuit board (Cockcroft-Walton base). A spring loaded mechanism guarantees good contact between the PMT and the light mixer while maintaining electrical contact with the base. The signals and services are provided through connectors and feedthrough on the backplane of the box where they are easily accessible, as illustrated in Fig. 5.25.

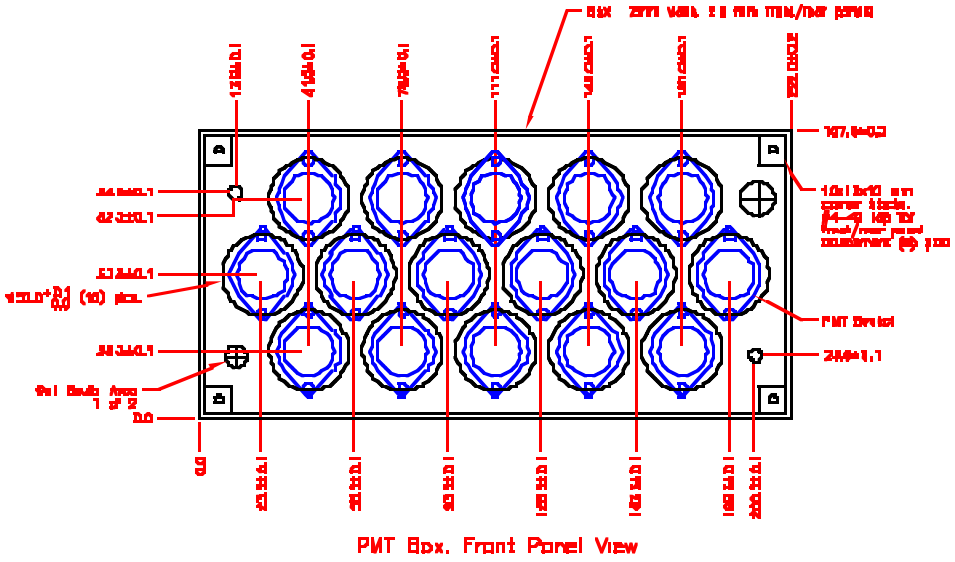

Fig. 5.25 (C. S.): The PMT box contains 16 PMTs and the Cockcroft-Walton high voltage generation components. The calibration and monitoring components for laser and LED are shown on the lower left and the upper right of the box. Two quick release screws position and mount the box onto the back of the steel shielding slab and are shown in upper left and lower right corners of the box.

5.7 ACCESS, MAINTENANCE AND OPERATIONS

5.7.1 Maintenance in the hall and garage

During assembly and periods of major maintenance or upgrade of the CMS detector, the HF calorimeters occupy garages at the experimental hall floor level at either end of the hall below the final focus quadrupoles. In the garage position the detector with its shielding rests on a transporter which is designed to move on airpads. The transporter consists of a steel structure mounted on four airpads with sufficient load bearing capacity to support the moving 310 tonne load of the detector and its shielding. Guide pins locate and secure the detector to the transporter. Locomotion between the garage and the location of the support structure is provided by winches. Guidance for the transporter in moving from garage to the support location is provided by steel cables attached to winches that are located in the garage.

The umbilical cord with the signal and power cables, the slow control cables, and the nitrogen purge and cooling water lines is constrained and moved in the 50×50 cm^2 utility trench by looping it in a pantograph arrangement similar to the UA2 detector at the SPS. At the detector the umbilicus splits into two bundles, one each for the left and right halves of the detector. The bundles enter the detector through the bottom front of the transporter platform and each bundle terminates at either of two racks (one high and one low) mounted on the shielding on either side of the detector.

A total of 15 cm is available below the platform and the floor. This space accommodates the cables, the main support structure, the components of the transverse drive mechanisms for the ±25 cm motion of the two halves of the detector, and the vertical fine-tuning mechanism to center the detector vertically on the beam. The main support structure, which rests on the transporter when the detector is in its low position, is capable of supporting the 310 tonne load of the shielded detector from the four outboard jacking points which have a transverse separation of 4.4 meters and a longitudinal separation of three meters. Placement of the umbilical connection at the front of the detector clears the space below the main support structure for insertion of the stacked support modules in the operational configuration at beam elevation.

The height of the detector and shield is 3.5 meters including the mounting base for the detector halves. This leaves about 1.5 meter of vertical clearance in the garage position, sufficient clearance for a limited crane structure. Maintenance of photomultiplier tubes and other electronics will be done in the garage, but major mechanical assembly and maintenance requiring substantial crane coverage will be carried out using the EH bridge crane or a portable gantry of appropriate capacity.

When the muon chambers and end cap calorimeter are in their retracted positions, the HF calorimeter is shielded in its garage by massive doors. When the muon chambers and end cap calorimeter are in their operational positions, the HF calorimeter can be serviced by the hall crane or a suitable portable gantry. Final shielding of the calorimeter is done at beam elevation using the hall crane.

While resting on the transporter in the low position, the main detector platform is less than 0.5 meter above the floor of the hall. This provides access to the lower electronics racks attached to the side of either half of the detector and to the PMT modules at the rear of the detector.

5.7.2 Radiation monitors

The HF will have to function in the worst radiation conditions of all CMS subdetectors. The estimated absorbed dose in the photomultipliers and read-out electronics during the lifetime of experiment is close to the upper limits for these devices. Therefore, the close monitoring of the background flux is extremely important. Based upon the results of Monte-Carlo simulation, we choose to monitor at the following locations as identified in below Table 5.9.

Table 5. 9
Location and measures of the HF radiation monitors

Point number	Coordinates z (cm)	Coordinates *r* (cm)	Energy (neutrons)	Neutron flux ($1/cm^2s$)	Hadron flux (E>15 MeV) ($1/cm^2s$)	γ flux (E=1-3 MeV) ($1/cm^2s$)
1	1320	100	<15 MeV	3×10^6		
			>15 MeV	1×10^5	5×10^4	3×10^6
2	1400	100	<15 MeV	5×10^4		
			>15 MeV	1×10^3	2×10^4	3×10^4
3	1320	230	<15 MeV	1×10^3		
			>15 MeV	1×10^3	2×10^1	2×10^3

Point 1 is located in the area of fibre bundles (near the point where they enter the shielding). Point 2 is in the vicinity of the PMT boxes. Point 3 is at the electronics racks. This allows monitoring radiation conditions for all the critical HF elements. The same coordinates (*r* or z) will help to understand the efficiency of the radiation shielding of the calorimeter and give information on neutron, hadron, and γ containment. The measurements must be performed for both the HF+ and HF-.

These measurements are achieved using standard detectors manufactured by industry. The γ flux can be measured by small (0.8-1 cm diameter, 5.5-6.3 cm length) Geiger-Mueller counters. The possible choice is counters of SI series (SI-38G, SI-34G, SI-37G), which is sensitive to photons in the energy range 0.1-10 MeV with a rate up to 2×10^7 particles/cm^2 s. The Si semiconductor detectors are used to detect charged hadron background. They function well with hadron intensity up to 10^6 particles/cm^2 s.

Since neutrons (especially of the low energy) are the most damaging component of radiation background for PMTs and the read-out electronics, special attention must be paid to neutron flux measurements with the possibility to estimate the spectrum of neutrons.

The space inside radiation shielding is very limited. Therefore, detectors of the KNT series can be used for point 1. They are small (0.7 cm diameter and 7.1 cm length) fission chambers with 1-3 mg of fission material. These detectors work at the neutron rates up to 2×10^{10} neutrons/cm^2sec (KNT-8) with the lower threshold of neutron energy of 400 keV (KNT-7). In addition, B^{10} proportional chambers can be installed to the fission detectors for the points outside radiation shielding. The SNM-13 counters have a diameter of 0.8 cm and a length of 8.5 cm. These detectors work well neutron fluxes up to 5×10^6 neutrons/cm^2 s which exceeds the estimated neutron level in monitoring points 2 and 3 by at least two orders of

magnitude. The bare counter is expected to detect thermal neutrons, but if equipped with polyethylene moderators of 5", 8", and 10" diameter, it will be able to detect neutrons up to energy 7, 20, and 30 MeV correspondingly. Polyethylene moderators will allow to evaluate the neutron spectrum. All quoted detectors are able to work in high γ fluxes which ensures the reliability of measurements.

References

[1] P. Gorodetzky et al, NIM A361 (1995) 161.
[2] P. Gorodetzky, Rad. Phys. And Chem. 41 (1993) 253.

TABLE OF CONTENTS